SMALL MOLECULE CONJUGATION OF HSP70 INHIBITS NECROPTOSIS

APPROVED BY SUPERVISORY COMMITTEE

Supervising Professor: Zhigao Wang, Ph.D. _____

Chairperson: Michael Roth, Ph.D. _____

Chuo Chen, Ph.D. _____

Peter Douglas, Ph.D. _____

DEDICATION

This work is dedicated to my mother, Sue A. Johnston, who taught me the value of education and perseverance.

SMALL MOLECULE CONJUGATION OF HSP70 INHIBITS NECROPTOSIS

by

ANDREA N. JOHNSTON

DISSERTATION

Presented to the Faculty of the Graduate School of Biomedical Sciences

The University of Texas Southwestern Medical Center at Dallas

In Partial Fulfillment of the Requirements

For the Degree of

DOCTOR OF PHILOSOPHY GENETICS, DEVELOPMENT, AND DISEASE

The University of Texas Southwestern Medical Center at Dallas

Dallas, Texas

August 2018

NOVEL COMPOUND NBC1 BLOCKS NECROPTOSIS THROUGH CONJUGATION OF HEAT SHOCK PROTEIN 70

Andrea N. Johnston, D.V.M., Ph.D.

The University of Texas Southwestern Medical Center at Dallas, 2018

Supervising Professor: Zhigao Wang, Ph.D.

Necroptosis is a subtype of regulated necrosis in which signaling through receptor interacting protein kinase 3 (RIPK3) triggers caspase independent, immunogenic cell death morphologically identical to necrosis. Necroptosis is physiologically relevant in viral disease, ischemia reperfusion injury, necrotizing pancreatitis, and systemic inflammatory response syndrome. Although many necroptotic stimuli exist, our research focuses on TNF mediated necroptosis. Following TNF-TNFR1 binding and concurrent inhibition of caspase 8, Receptor Interacting Protein Kinase 1 and 3 (RIPK1/3) bind through their Receptor Homotypic Interacting Motif (RHIM) domains, activate via phosphorylation, and form an amyloid-like structure termed the necrosome. RIPK3 recruits and phosphorylates Mixed Lineage Kinase-Like (MLKL) protein. This induces MLKL polymerization, which putatively causes direct cell membrane disruption resulting in cell death. The steps downstream of the MLKL phosphorylation remain poorly defined. We designed and carried out a forward small molecule screen, which identified an inhibitor of necroptosis (Necroptosis Blocking Compound 1, NBC1) downstream of MLKL phosphorylation. Positive, negative, and biotinylated analogs of this compound led to identification of the drug target (Hsp70) by LC-MS. Biochemical data suggests that NBC1 conjugates Hsp70 and blocks necroptosis by inhibiting MLKL polymerization.

TABLE OF CONTENTS

PRIOR PUBLICATIONS

Liu S, Liu H, **Johnston A**, Hanna-Addams S, Reynoso E, Xiang Y, Wang Z. MLKL forms disulfide bond-dependent amyloid-like polymers to induce necroptosis. Proc Natl Acad Sci U S A. 2017 Sep 5;114(36):E7450-E7459. PMID: 28827318

Davignon DL, Lee AC, **Johnston AN**, Bowman DD, Simpson KW. Evaluation of capsule endoscopy to detect mucosal lesions associated with gastrointestinal bleeding in dogs. J Small Anim Pract. 2016 Mar;57(3):148-58. PMID: 26931500

Webster CR, **Johnston AN**, Anwer MS. Protein kinase Cδ protects against bile acid apoptosis by suppressing proapoptotic JNK and BIM pathways in human and rat hepatocytes. Am J Physiol Gastrointest Liver Physiol. 2014 Dec 15; 307(12):G1207-15. PMID: 25359536

Johnston A, Center S, McDonough S, Wakshlag J, Warner K. Hepatic copper concentrations in Labrador Retrievers with and without chronic hepatitis (1980-2010): increased liver copper implicates increased dietary exposure. Journal of the American Veterinary Medical Association. 2013; 242(3):372-80. PMID: 23327181

Abelson A, O'Toole T, **Johnston A**, Respess M, de Laforcade A. Hypoperfusion and Acute Traumatic Coagulopathy in Severely Traumatized Canine. Journal of Veterinary Emergency and Critical Care. 2013 Jul-Aug;23(4):395-401. PMID: 23855637

Respess M, O'Toole T, Taeymans O, Rogers C, **Johnston A**, Webster C. Portal vein thrombosis in 33 dogs: 1998 – 2011. Journal of Veterinary Internal Medicine. 2012; 26(2):230-7. PMID: 22369249

Johnston A, Ponzetti K, Anwer MS, Webster CR. cAMP-guanine exchange factor protection from bile acid induced hepatocyte apoptosis involves glycogen synthase kinase regulation of C-Jun-NH terminus kinase. American Journal of Physiology. Gastrointestinal and Liver Physiology. 2011; 301(2):G385-400. Epub 2011 May 5. PMID: 21546580

Buob S, **Johnston AN**, Webster CR. Portal hypertension: pathophysiology, diagnosis, and treatment. Journal of Veterinary Internal Medicine. 2011; 25(2):169-86. PMID:21382073

Johnston AN, Center SA, McDonough SP, Warner KL Influence of biopsy size, tissue fixation, and assay variation on copper, iron, and zinc concentrations in canine liver. American Journal of Veterinary Research. 2009;70(12):1502-11. PMID: 19951122

LIST OF FIGURES

Chapter 1. Introduction

Chapter 2. The subcellular localization of MLKL and identification of the MLKL polymer by negative staining Electron Microscopy

Chapter 3. Necroptosis blocking compound 1 (NBC1) inhibits necroptosis by conjugating Heat shock protein 70 and abrogating MLKL polymerization

LIST OF ABBREVIATIONS

4-helix bundle domain (4HBD)

Apoptosis signal-regulating kinase 1 (ASK1)

β-mercaptoethanol (βME)

Cellular inhibitors of apoptosis (cIAPs)

Damage-associated molecular patterns (DAMPs)

Death domain (DD)

Death-inducing signaling complex (DISC)

Dithiothreitol (DTT)

Doxycycline (Dox)

Fas ligand receptor (FasL)

FAS-associated death domain protein (FADD)

Heat shock protein 70 (Hsp70)

Heat shock protein 90 (Hsp90)

Herpes Simplex Virus types 1 and 2 (HSV-1/2)

High mobility group box 1 protein (HMGB1)

Mixed lineage kinase domain-like pseudokinase (MLKL)

MLKL N-terminus domain (NTD)

Necrostatin-1 (Nec-1)

Necrosulfonamide (NSA)

Nucleotide binding domain of Hsp70 (NBD)

Phosphatidylinositol phospholipids (PIPs)

Receptor homotypic interaction motif (RHIM)

Receptor interacting protein kinase 1 (RIPK1)

Receptor interacting protein kinase 3 (RIPK3)

Regulated cell death (RCD)

Semi-denaturing detergent agarose gel electrophoresis (SDD-AGE)

Substrate binding domain of Hsp70 (SBD)

Thioredoxin-1 (Trx1)

TNF receptor 1 (TNFR1)

TNF-related apoptosis-inducing ligand receptor 1/2 (TRAILR1/2)

Toll-like receptors 3 and 4 (TLR3/4)

Tumor necrosis factor receptor type 1-associated death domain protein (TRADD)

Z-DNA binding protein 1 (ZBP1)

CHAPTER ONE
Introduction

Regulated cell death

Elimination of impaired, harmful, or redundant cells is essential to biologic homestasis.[1] Unless the cell is overcome by severe chemical, osmotic, or mechanical stress, resulting in accidental cell death, then a genetically encoded cell death pathway ensues. Molecularly signaled cell death falls into two large categories, physiologic and pathologic. The former, referred to as programmed cell death, is requisite during development and tissue turnover. Whereas, pathologic regulated cell death (RCD) occurs when endogenous or exogenous stimuli trigger specific signal transduction cascades causing cell death. Apoptosis, the first RCD pathway identified, fits into both groups.[2-4] Extensive investigation of apoptosis determined that the process was controlled by a tightly regulated set of molecular signals and dependent on caspase activity. Detailed understanding of apoptosis has led to discovery of other RCD pathways. [5,6]

The list of RCD pathways has expanded dramatically over the past two decades. A recent publication of the Nomenclature Committee on Cell Death has reclassified RCD pathways based on molecular mechanisms rather than morphologic characteristics.[1] In addition to apoptosis, RCD subroutines include necroptosis (discussed in detail below), parthanatos initiated by massive genomic stress, pyroptosis caused by pathogen invasion and culminating in plasma membrane pore formation by the gasdermin protein family, ferroptosis stimulated by

intracellular oxidative perturbations such as severe lipid peroxidation and dependent on iron availability, and mitochondrial permeability transition (MPT) driven necrosis.[7-12] Additionally, multiple phagocytic and lysosome dependent cell death processes have been described: autophagy-dependent cell death, autosis, entosis, and lysosome-dependent cell death.[1,13] The large number of cell death pathways may reflect the critical regulatory importance of single cell elimination to promote organismal health.

Necroptosis is a subtype of regulated necrosis that occurs when caspases are inhibited or fail to activate. Stimulus of cell death receptors results in a signaling cascade that triggers caspase independent, kinase dependent, immunogenic cell death.[14] Phenotypically, necroptosis is indistinguishable from necrosis, identified by organelle swelling, loss of plasma membrane integrity, and release of cytoplasmic contents including pro-inflammatory mediators or damage associated molecular patterns (DAMPs). These include ATP, the chromatin-associated protein high-mobility group box 1 HMGB1, and mitochondrial DNA, which induce an innate inflammatory response. Gong *et al.* identified an additional means of pro-inflammatory signaling secondary to necroptosis, wherein ESCRT-III facilitates shedding of the MLKL-damaged plasma membrane from intact cells. These secretory “bubbles” not only stimulate a local immune response but also sustain cellular integrity.[15]

Necroptotic cell death has been described in TNF-mediated systemic inflammatory response syndrome (SIRS), ischemic reperfusion injury,

neurodegeneration, and pathogen infection, particularly viral disease.[16-19] Yet, it is increasingly clear that programmed cell death in infectious and non-infectious disease states is unlikely to be unilateral. Many pathways share common signaling components and effector mechanisms. Recent evidence suggests that multiple parallel cell death pathways may be occurring concurrently.[20-23] The overlap complicates understanding of RCD in disease and can confound pharmacologic targeting strategies.

TNF-mediated necroptosis

Induction of necroptosis results from physiologic or pathophysiologic stimuli. Cell extrinsic signals of necroptosis include ligands of the death receptor family (TNF, FAS or TRAIL), viral double stranded DNA or lipopolysaccharide stimulation of TLR 3 and 4, respectively, inflammatory mediators like interferon and viral stimulus of DNA-dependent activator of interferon regulatory factor.[21,24] The best studied is TNF-mediated necroptosis. The death receptors of the TNF family contain a cytoplasmic death domain (DD). Ligand binding to the death receptor TNFR1 induces receptor trimerization. This conformational change enhances binding with the DD adaptor proteins Receptor Interacting Protein Kinase (RIPK1) and TNF receptor-associated DD (TRADD), forming complex I. RIPK1 is a hub for multiple cell stress signaling cascades. RIPK1 consists of an N-terminus kinase domain, intermediary domain, and a C-terminus RHIM domain and death domain. RIPK1 is ubiquitylated in its intermediate domain, recruiting the IκB complex. IKKα and IKKß phosphorylate RIPK1, preventing its dissociation and leading to cell survival through

inflammatory cytokine signaling. RIPK1 kinase activity is not necessary for the pro-survival NF-κB pathway, unlike for the cell death pathways.[25]

When ubiquitylation of RIPK1 is disrupted through loss of the E3 ligases,[26] cell death signaling proceeds with formation of complex IIa or IIb.[27] Subsequently, three cell death outcomes are possible: necroptosis, RIPK1-dependent and independent apoptosis.[28] Complex IIa is formed when TRADD dissociates from TNFR1, leading to recruitment of FADD, activation of caspase 8, and RIPK1 independent apoptosis. If cIAPs, TAK1, or IKKα/ß are absent or inhibited, complex IIb including RIPK1, FADD, cFLIP, and caspase 8 is formed and results in RIPK1 dependent apoptosis (Fig. 1.1A).[25]

Of the cell death pathways, apoptosis predominates when caspase 3 and 8 are active, and necroptosis progresses when caspase activity is absent or inactivated, but recent evidence suggests that caspase inhibition is not imperative for necroptosis and both cell death pathways can progress concurrently dependent on cellular context.[29] The fate decision to proceed towards necroptosis is dictated by TAK1 phosphorylation of Ser231 in the intermediate domain of RIPK1.[30]

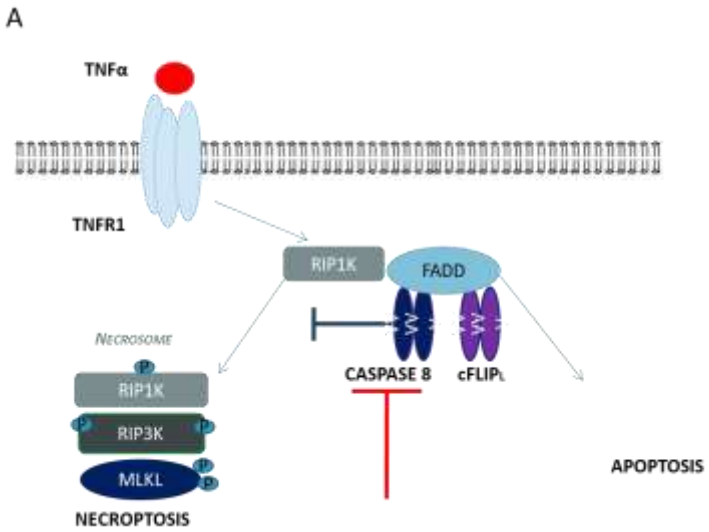

Figure 1.1. (A) Schematic representation of TNF-TNFR1 cell death signaling.

The core pathway

In the canonical necroptosis pathway, consists of two kinases, RIPK1 and RIPK3, and one pseudokinase, MLKL. Following death receptor stimulation and sustained phosphorylation of the intermediate domain of RIPK1, interaction with RIPK3 occurs, as long as RIPK3 intracellular level is sufficient.[14,31] RIPK1 binds RIPK3, a homologous serine/threonine kinase, through their C-terminus Receptor Homotypic Interacting Motif (RHIM) domains. RIPK3 has an N-terminus kinase domain, intermediate domain, and a C-terminus RHIM domain but lacks a DD. Like RIPK1, RIPK3 is a pleiotropic kinase. Aside from necroptosis, RIPK3 is linked to inflammasome activation, apoptosis, and intestinal tissue regeneration.[32-34] RIPK3 is activated by phosphorylation. RIPK1 kinase activity was initially believed responsible for RIPK3 phosphorylation but other kinases, including RIPK3 itself, may be

involved. RIPK3 activation via phosphorylation is imperative to necroptosis and seeds synthesis of an amyloid-like oligomer termed the necrosome.[35,36]

RIPK3 recruits Mixed Lineage Kinase domain-Like pseudokinase (MLKL), the obligatory effector of necroptosis, to the necrosome.[37] MLKL binds RIPK3 through its kinase-like domain.[38] Phosphorylation of RIPK3 Ser227 is required for MLKL interaction.[39] RIPK3 phosphorylation of MLKL triggers a conformational shift, leading to MLKL release from the necrosome, and necroptotic cell death.[25]

Alternative RIPK1-independent, RIPK3-dependent necroptotic pathways have been described. RIPK3 can be activated through RHIM domain-containing adaptor TRIF, functioning downstream of TLR3/4, or Z-DNA sensor DAI (ZBP1/DAI).[40] RIPK1 binding blocks the RIPK3 and ZBP1/DAI mediated necroptosis.[41]. RIPK3-independent activation of MLKL has recently been described in a model of acute inflammatory hepatitis induced by concanavalin A.[42] This opens the door to other potential direct MLKL stimuli. A second RIPK3 substrate, calcium-dependent protein kinase II delta (CAMK2D) may also be involved in cell death.[42] RIPK3 activates CAMK2D through phosphorylation of Thr387. CAMK2D regulates multiple ion channels, its phosphorylation results in an influx of extracellular ions. This occurs independently of MLKL and the exact relationship between CAMK2D and necroptosis is uncertain.

The structural regulation of mixed lineage kinase domain like pseudokinase (MLKL)

MLKL has two functional domains, the N-terminus four-helix bundle (4HB) and a C-terminus pseudokinase domain linked by two helices, termed the brace domain. The 4HB domain is composed of residues 1-124 in humans and 1-125 in mice. The structure of full-length mouse MLKL was solved by X-ray crystallography and human N-terminus domain (NTD, residues 1-154) by NMR.[43,44] Both species share a common 4HB core. In mice the second and fourth helices are packed against the N-terminus portion of the first brace helix and this interaction is likely dynamic. In the human NMR structure, an additional helix was identified between helix 3 and 4 that caps one end of the bundle. The brace helices tethering the 4HB to the pseudokinase domain transmit pseudokinase domain phosphorylation events to the N-terminus 4HB and inducing conformational changes and promoting cell execution.[45]

MLKL evolved as a pseudokinase, rather than an active kinase.[46,47] Typically, kinases have a conserved structure. The N-terminus contains five antiparallel β-strands and one α-helix, which packs against the larger C-terminus domain almost entirely composed of α helices. In active protein kinases three motifs are conserved: VAIK, important for ATP positioning; HRD in the catalytic loop; and the DFG in the activation loop to bind $Mg^{2+,}$ which coordinates β and γ-phosphates of the ATP molecule. MLKL's pseudokinase domain lacks key residues necessary for phosphoryl transfer making it catalytically dead.[37,44] In most species, MLKL retains the VAIK but not the HRD motif and the DFG motif is highly variable.[46] MLKL can

bind ATP despite the absence of hydrolytic activity but the biologic function of this is unknown.[48]

The murine activation loop (residues 340-346) adopts the α helical structure of an active protein kinase; however, K219 interacts with conserved residue Q343, which is atypical for an active kinase. When either residue is mutated to Ala, necroptosis is triggered in the absence of stimuli.[44] RIPK3 phosphorylates S345, S347, and T349 in mouse MLKL and S345 is the key trigger for MLKL activation. Human activation loop (residues 357-368) is phosphorylated at T357 and S358.[37,49] Alanine mutagenesis of these sites blocks necroptosis.[37] Additional phosphorylation sites have been found in humans and mice. Mutation of S158 or S248 to alanine (phospho-ablating) but not glutamate or aspartate (phosphomimetic) in mice led to necroptotic cell death without stimuli. Therefore, the pseudokinase domain is implicated as a suppressor of necroptotic death.[50]

The N-terminus 4HB is the executioner domain. Inducible expression of the 4HB causes cell death in the absence of stimuli. The 4HB does not share significant sequence or structural homology to other protein families, making its mechanistic function difficult to deduce.[21] Mutational analysis of mouse 4HB indicated that residues critical for cell death were clustered in two regions on opposing faces of the 4HB. The first cluster localized on α-helices 3 (R63/D65) and 4 (E102/K103, R105/D106, E109/E110, and L112/L115) composed principally of poorly conserved acidic residues and the second cluster on the α-helices 1 (Y15/E16) and 2 (C18/C24/C28). Cluster one mutations completely inhibited membrane translocation,

high molecular weight MLKL complex formation, and cell death. Cluster two mutations were dispensable for translocation and high molecular weight complex formation, but prevented cell death.[50] These data suggest that although membrane translocation and polymerization alone are insufficient to cause cell death. Yet exactly how MLKL permeabilizes the membrane remains uncertain. Proposed mechanisms include partial insertion of the 4HB into the plasma membrane, association with or generation of transmembrane ion channels to induce osmolysis, or intramembrane oligomerization leading to mechanical membrane disruption.[21,50-53]

Polymerization of MLKL

Upon phosphorylation of MLKL by RIPK3, MLKL undergoes a conformational change that triggers MLKL oligomerization.[40,43,47,50,52-54] The presence of the brace region is critical to formation of MLKL dimers, trimers, and tetramers as human MLKL 1-140 lacking the brace region remains monomeric, yet residues 1-125 in mouse MLKL lacking the brace region can kill fibroblasts.[43,50,55] MLKL octamer formation has been shown to occur at the necrosome and precedes MLKL dissociation from the necrosome and translocation to the plasma membrane.[56] The structural stability of octameric MLKL does not require disulfide bonds but polymeric MLKL relies on intermolecular disulfide bonds.[54,56] Under steady-state conditions, the cytoplasmic thiol oxidoreductase thioredoxin-1 (Trx1) system maintains cellular redox balance by catalyzing disulfide exchange reactions, to limit disulfide bond

formation between target proteins, such as monomeric MLKL. The small molecule necroptosis inhibitor, enhances this interaction by cross-linking Trx1 cysteine-32 to cysteine-86 of human MLKL which blocks MLKL polymerization and membrane permeabilization.[57] When cellular homeostatic mechanisms such as the Trx1 system are overwhelmed or inhibited, necroptosis ensues. It is agreed that MLKL phosphorylation, membrane translocation, and oligomerization are necessary for necroptosis, but the specific mechanisms of these downstream steps and exactly how LKL causes membrane permeabilization is unresolved. The objective of our research is to identify additional protein mediators integral to the terminus steps of necroptosis.

References

1. Galluzzi, L.*, et al.* Molecular mechanisms of cell death: recommendations of the Nomenclature Committee on Cell Death 2018. *Cell Death Differ* **25**, 486-541 (2018).
2. Thornberry, N.A. Caspases: key mediators of apoptosis. *Chem Biol* **5**, R97-103 (1998).
3. Lazebnik, Y.A., Takahashi, A., Poirier, G.G., Kaufmann, S.H. & Earnshaw, W.C. Characterization of the execution phase of apoptosis in vitro using extracts from condemned-phase cells. *J Cell Sci Suppl* **19**, 41-49 (1995).
4. Kerr, J.F., Wyllie, A.H. & Currie, A.R. Apoptosis: a basic biological phenomenon with wide-ranging implications in tissue kinetics. *Br J Cancer* **26**, 239-257 (1972).
5. Wang, C. & Youle, R.J. The role of mitochondria in apoptosis*. *Annu Rev Genet* **43**, 95-118 (2009).
6. Liu, X., Kim, C.N., Yang, J., Jemmerson, R. & Wang, X. Induction of apoptotic program in cell-free extracts: requirement for dATP and cytochrome c. *Cell* **86**, 147-157 (1996).
7. Fink, S.L. & Cookson, B.T. Apoptosis, pyroptosis, and necrosis: mechanistic description of dead and dying eukaryotic cells. *Infect Immun* **73**, 1907-1916 (2005).

8. Fink, S.L. & Cookson, B.T. Caspase-1-dependent pore formation during pyroptosis leads to osmotic lysis of infected host macrophages. *Cell Microbiol* **8**, 1812-1825 (2006).
9. Bergsbaken, T., Fink, S.L. & Cookson, B.T. Pyroptosis: host cell death and inflammation. *Nat Rev Microbiol* **7**, 99-109 (2009).
10. Vanden Berghe, T., Linkermann, A., Jouan-Lanhouet, S., Walczak, H. & Vandenabeele, P. Regulated necrosis: the expanding network of non-apoptotic cell death pathways. *Nat Rev Mol Cell Biol* **15**, 135-147 (2014).
11. Xie, Y.*, et al.* Ferroptosis: process and function. *Cell Death Differ* **23**, 369-379 (2016).
12. David, K.K., Andrabi, S.A., Dawson, T.M. & Dawson, V.L. Parthanatos, a messenger of death. *Front Biosci (Landmark Ed)* **14**, 1116-1128 (2009).
13. Tasdemir, E.*, et al.* Methods for assessing autophagy and autophagic cell death. *Methods Mol Biol* **445**, 29-76 (2008).
14. He, S.*, et al.* Receptor interacting protein kinase-3 determines cellular necrotic response to TNF-alpha. *Cell* **137**, 1100-1111 (2009).
15. Gong, Y.N.*, et al.* ESCRT-III Acts Downstream of MLKL to Regulate Necroptotic Cell Death and Its Consequences. *Cell* **169**, 286-300 e216 (2017).
16. Duprez, L.*, et al.* RIP kinase-dependent necrosis drives lethal systemic inflammatory response syndrome. *Immunity* **35**, 908-918 (2011).
17. Adameova, A.*, et al.* Evidence of necroptosis in hearts subjected to various forms of ischemic insults. *Can J Physiol Pharmacol*, 1-7 (2017).
18. Orozco, S. & Oberst, A. RIPK3 in cell death and inflammation: the good, the bad, and the ugly. *Immunol Rev* **277**, 102-112 (2017).
19. Fan, J., Dawson, T.M. & Dawson, V.L. Cell Death Mechanisms of Neurodegeneration. *Adv Neurobiol* **15**, 403-425 (2017).
20. Mocarski, E.S., Kaiser, W.J., Livingston-Rosanoff, D., Upton, J.W. & Daley-Bauer, L.P. True grit: programmed necrosis in antiviral host defense, inflammation, and immunogenicity. *J Immunol* **192**, 2019-2026 (2014).
21. Petrie, E.J., Hildebrand, J.M. & Murphy, J.M. Insane in the membrane: a structural perspective of MLKL function in necroptosis. *Immunol Cell Biol* **95**, 152-159 (2017).
22. Galluzzi, L., Kepp, O., Chan, F.K. & Kroemer, G. Necroptosis: Mechanisms and Relevance to Disease. *Annu Rev Pathol* **12**, 103-130 (2017).
23. Chien, H. & Dix, R.D. Evidence for multiple cell death pathways during development of experimental cytomegalovirus retinitis in mice with retrovirus-induced immunosuppression: apoptosis, necroptosis, and pyroptosis. *J Virol* **86**, 10961-10978 (2012).
24. Holler, N.*, et al.* Fas triggers an alternative, caspase-8-independent cell death pathway using the kinase RIP as effector molecule. *Nat Immunol* **1**, 489-495 (2000).

25. Grootjans, S., Vanden Berghe, T. & Vandenabeele, P. Initiation and execution mechanisms of necroptosis: an overview. *Cell Death Differ* **24**, 1184-1195 (2017).
26. Vasilikos, L., Spilgies, L.M., Knop, J. & Wong, W.W. Regulating the balance between necroptosis, apoptosis and inflammation by inhibitors of apoptosis proteins. *Immunol Cell Biol* **95**, 160-165 (2017).
27. Wang, L., Du, F. & Wang, X. TNF-alpha induces two distinct caspase-8 activation pathways. *Cell* **133**, 693-703 (2008).
28. Micheau, O. & Tschopp, J. Induction of TNF receptor I-mediated apoptosis via two sequential signaling complexes. *Cell* **114**, 181-190 (2003).
29. Nogusa, S.*, et al.* RIPK3 Activates Parallel Pathways of MLKL-Driven Necroptosis and FADD-Mediated Apoptosis to Protect against Influenza A Virus. *Cell Host Microbe* **20**, 13-24 (2016).
30. Geng, J.*, et al.* Regulation of RIPK1 activation by TAK1-mediated phosphorylation dictates apoptosis and necroptosis. *Nat Commun* **8**, 359 (2017).
31. Zhang, D.W.*, et al.* RIP3, an energy metabolism regulator that switches TNF-induced cell death from apoptosis to necrosis. *Science* **325**, 332-336 (2009).
32. Newton, K.*, et al.* Activity of protein kinase RIPK3 determines whether cells die by necroptosis or apoptosis. *Science* **343**, 1357-1360 (2014).
33. Lawlor, K.E.*, et al.* RIPK3 promotes cell death and NLRP3 inflammasome activation in the absence of MLKL. *Nat Commun* **6**, 6282 (2015).
34. Moriwaki, K. & Chan, F.K. The Inflammatory Signal Adaptor RIPK3: Functions Beyond Necroptosis. *Int Rev Cell Mol Biol* **328**, 253-275 (2017).
35. Li, J.*, et al.* The RIP1/RIP3 necrosome forms a functional amyloid signaling complex required for programmed necrosis. *Cell* **150**, 339-350 (2012).
36. Mompean, M.*, et al.* The Structure of the Necrosome RIPK1-RIPK3 Core, a Human Hetero-Amyloid Signaling Complex. *Cell* (2018).
37. Sun, L.*, et al.* Mixed lineage kinase domain-like protein mediates necrosis signaling downstream of RIP3 kinase. *Cell* **148**, 213-227 (2012).
38. Shan, B., Pan, H., Najafov, A. & Yuan, J. Necroptosis in development and diseases. *Genes Dev* **32**, 327-340 (2018).
39. Xie, T.*, et al.* Structural insights into RIP3-mediated necroptotic signaling. *Cell Rep* **5**, 70-78 (2013).
40. Dondelinger, Y.*, et al.* MLKL compromises plasma membrane integrity by binding to phosphatidylinositol phosphates. *Cell Rep* **7**, 971-981 (2014).
41. Vanden Berghe, T. & Kaiser, W.J. RIPK1 prevents aberrant ZBP1-initiated necroptosis. *Oncotarget* **8**, 1-2 (2017).
42. Zhang, T.*, et al.* CaMKII is a RIP3 substrate mediating ischemia- and oxidative stress-induced myocardial necroptosis. *Nat Med* **22**, 175-182 (2016).
43. Su, L.*, et al.* A plug release mechanism for membrane permeation by MLKL. *Structure* **22**, 1489-1500 (2014).

44. Davies, K.A.*, et al.* The brace helices of MLKL mediate interdomain communication and oligomerisation to regulate cell death by necroptosis. *Cell Death Differ* (2018).
45. Czabotar, P.E. & Murphy, J.M. A tale of two domains - a structural perspective of the pseudokinase, MLKL. *FEBS J* **282**, 4268-4278 (2015).
46. Tanzer, M.C.*, et al.* Evolutionary divergence of the necroptosis effector MLKL. *Cell Death Differ* **23**, 1185-1197 (2016).
47. Murphy, J.M.*, et al.* The pseudokinase MLKL mediates necroptosis via a molecular switch mechanism. *Immunity* **39**, 443-453 (2013).
48. Murphy, J.M.*, et al.* Insights into the evolution of divergent nucleotide-binding mechanisms among pseudokinases revealed by crystal structures of human and mouse MLKL. *Biochem J* **457**, 369-377 (2014).
49. Wang, H.*, et al.* Mixed lineage kinase domain-like protein MLKL causes necrotic membrane disruption upon phosphorylation by RIP3. *Mol Cell* **54**, 133-146 (2014).
50. Hildebrand, J.M.*, et al.* Activation of the pseudokinase MLKL unleashes the four-helix bundle domain to induce membrane localization and necroptotic cell death. *Proc Natl Acad Sci U S A* **111**, 15072-15077 (2014).
51. Hildebrand, J.M., Lucet, I.S. & Murphy, J.M. Flicking the molecular switch underlying MLKL-mediated necroptosis. *Mol Cell Oncol* **2**, e985550 (2015).
52. Cai, Z.*, et al.* Plasma membrane translocation of trimerized MLKL protein is required for TNF-induced necroptosis. *Nat Cell Biol* **16**, 55-65 (2014).
53. Chen, X.*, et al.* Translocation of mixed lineage kinase domain-like protein to plasma membrane leads to necrotic cell death. *Cell Res* **24**, 105-121 (2014).
54. Liu, S.*, et al.* MLKL forms disulfide bond-dependent amyloid-like polymers to induce necroptosis. *Proc Natl Acad Sci U S A* (2017).
55. Quarato, G.*, et al.* Sequential Engagement of Distinct MLKL Phosphatidylinositol-Binding Sites Executes Necroptosis. *Mol Cell* **61**, 589-601 (2016).
56. Huang, D.*, et al.* The MLKL Channel in Necroptosis Is an Octamer Formed by Tetramers in a Dyadic Process. *Mol Cell Biol* **37**(2017).
57. Reynoso, E.*, et al.* Thioredoxin-1 actively maintains the pseudokinase MLKL in a reduced state to suppress disulfide bond-dependent MLKL polymer formation and necroptosis. *J Biol Chem* (2017).

CHAPTER TWO
The subcellular localization of MLKL and identification of the MLKL polymer by negative staining electron microscopy

Introduction

Although disruption of the plasma membrane by MLKL is the currently favored model of necroptotic cell death, this may not be the only cellular membrane targeted *in vivo*.[1-6] MLKL's binding affinity for negatively charged phospholipids has been explored in multiple *in vitro* studies.[2,3,5,7] Using hydrophobic membrane lipid strips and lipid binding assays, MLKL's binding predilection included phosphoinositide species and the inner mitochondrial membrane specific cardiolipin.[2,5] Phosphoinositides are acidic phospholipids that interact with proteins and regulate integral membrane proteins.[8] Phosphoinositide species are specific to each cellular compartment membrane. MLKL's phosphoinositide binding repertoire included phosphatidylinositol 4-phosphate (PI(4)P, trans Golgi), phosphatidylinositol (4,5)-bisphosphate ($PI(4,5)P_2$, plasma membrane), phosphatidylinositol (3,4,5)-triphosphate (PIP_3, plasma membrane), phosphatidylinositol (3)-phosphate (PI(3)P, late endosome and multivesicular bodies), phosphatidylinositol (3,4)-biphosphate ($PI(3,4)P_2$, early endosome), and phosphatidylinositol (3,5)-biphosphate ($PI(3,5)P_2$, late endosome).[3,5] MLKL's diverse organelle membrane binding was validated through cell fractionation experiments and immunostaining.[3] MLKL binding to plasma membrane PI(4,5)P2 is widely accepted as causal to cell death in necroptosis,[1,7] but the importance of MLKL's affinity for the other phosphoinositides and cardiolipin remains unclear. Initially, the mitochondria was believed to play a role

in necroptosis,[9] however, multiple studies have downplayed the its significance and it is generally considered dispensable for necroptotic cell death.[1,10-13]

Recombinant full length and N-terminus MLKL were capable of inducing leakage of PI(4,5)P2 containing liposomes, and this occurred more efficiently than liposomes mimicking the mitochondrial membrane.[2,5] Although the N-terminus of MLKL was capable of disrupting liposomes, it was not able to disrupt nanodiscs, which have a more rigid membrane surface structure due to the presence of a scaffolding protein.[2,3,8] This supports insertion of the N-terminus 4HB, at least partially, into the lipid membranes, and this insertion may be stabilized by the pseudokinase region.[7,14-17] Whether this insertion causes direct cell membrane disruption *in vivo* or invokes a secondary response remains contentious. $PI(4,5)P_2$ attracts proteins associated with membrane budding and fusion and regulates ion channels.[8] Evidence exists to support MLKL's membrane permeabilization through formation of cation channels or association with existing ion channels;[4,7,18,19] however, conformation and structural imaging has not yet identified the plasma membrane permeating structure.

While other labs have documented MLKL's migration to the plasma membrane following necroptosis induction using confocal microscopy, the Wang laboratory has not been able to reproduce this data.[20] It is unclear whether this is due to the use of different reagents, cell lines, or experimental techniques, or in fact represents true experimental finding. Therefore, we sought to use an alternative technique, immunogold transmission electron microscopy, to investigate the

subcellular localization of MLKL after necroptosis induction. Secondarily, we wanted to determine if the large oligomeric form of MLKL identified biochemically could be a structured amyloid-like fiber similar to the RIPK1-RIPK3 fibers identified by Li et al using negative stain transmission electron microscopy.[21,22]

Results

Subcellular localization of MLKL by immunogold transmission electron microscopy.

Cytoplasmic MLKL punctae are detectable in cells undergoing necoptosis with confocal microscopy (Fig. 2.1A). To determine subcellular localization of MLKL after necroptosis induction immunogold labelling was undertaken. NTD-DmrB cells were plated on gridded glass coverslips and necroptosis was induced with dimerizer and ZVAD-FMK. Cells were fixed and Flag-NTD-MLKL was immunocytochemically labelled with M2 antibody and fluorescent (RFP) secondary antibody. RFP positive cells were assessed for morphologic characteristics of necroptosis and mapped to a specific grid region (Fig. 2.1B). With help from the UT Southwestern Electron Microscopy Core, these cells were embedded, labelled with immunogold beads targeting the secondary antibody, and imaged with transmission electron microscopy (Fig. 2.1C). This experiment was repeated three times but yielded incongruous results. Initially, immunogold beads targeted the plasma membrane (Fig. 2.1C, upper panels), consistent with consensus in the field, but later studies identified immunogold particles adhered to the mitochondria and cytoskeletal structure (Fig.

2.1C, lower panels). Due to the nature of cell death, which results in plasma membrane rupture, leakage of cytoplasmic contents, and cell detachment, technical difficulties were common. Necroptotic cells were often severely degraded (Fig. 2.1C, lower, right panel), and in some cases did not persist through the embedding process. Despite identically timed death induction, cells were rarely in uniform states of necroptotic death. Additionally, it was determined that under some conditions the M2 antibody non-specifically labels cytostructural elements, presumably actin filaments (Fig. 2.1D), invalidating its use in the immunogold assay.

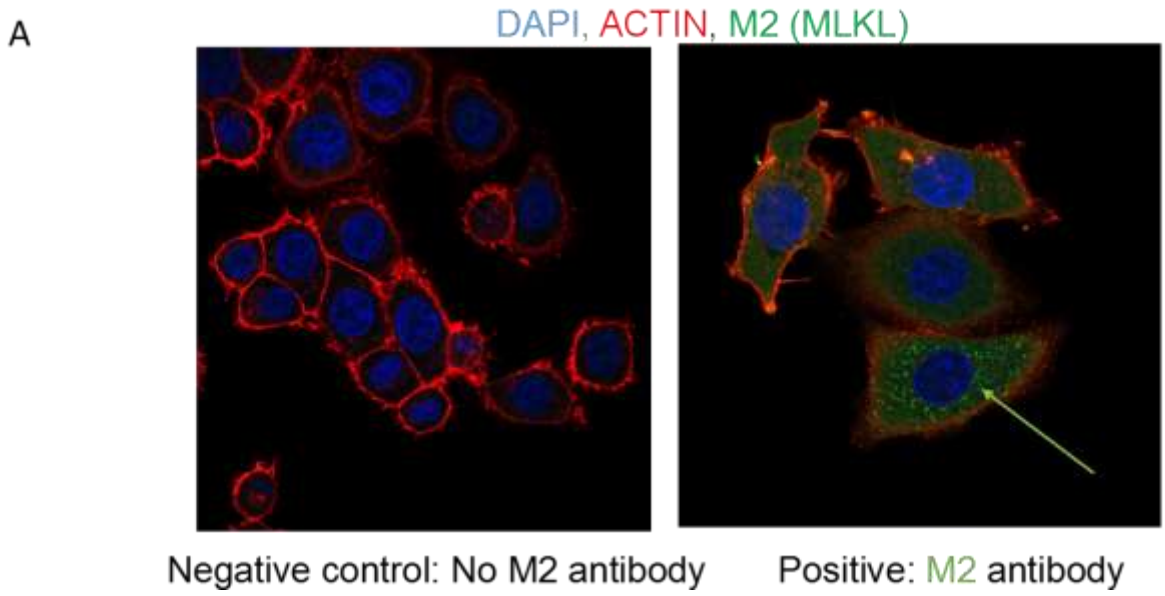

B

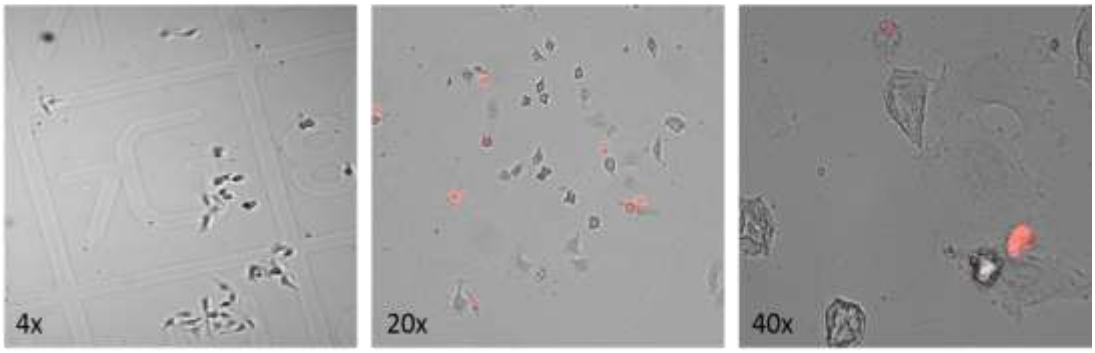

C

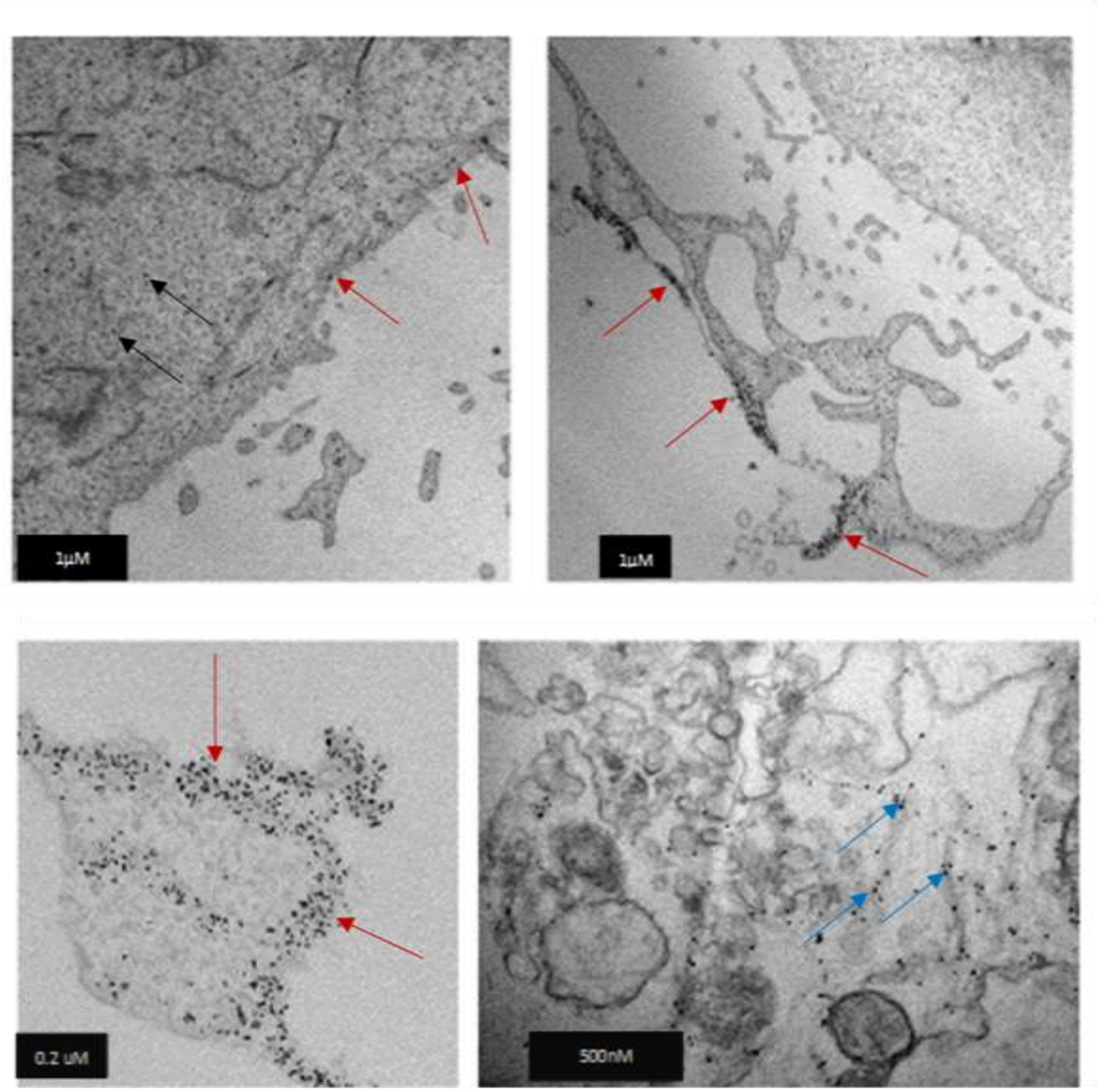

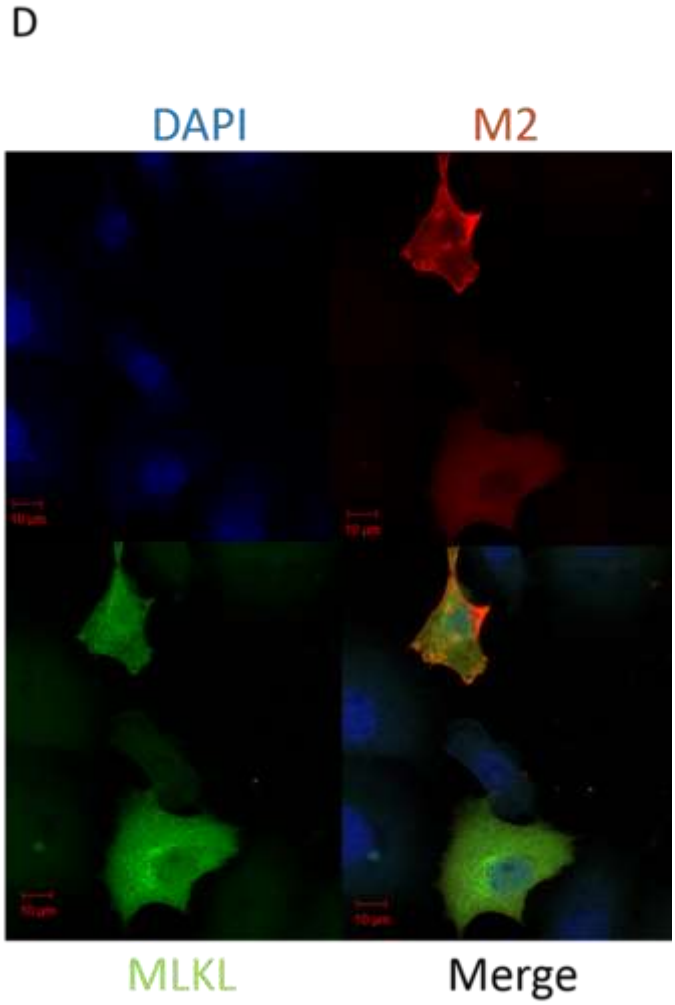

Figure 2.1 Immunogold subcellular localization of MLKL
(A) NTD-DmrB cells were plated on glass coverslips. Cells were treated with 20 nM dimerizer and 20 µM ZVAD-FMK. Cells were subjected to fixation and staining with M2 antibody (labelling Flag-MLKL) or no primary antibody (M2 (green)/Actin (red)/DAPI (blue) staining identified). Left panel control without primary M2 (MLKL) antibody and right panel shows diffuse MLKL in cytoplasm in top three cells and MLKL foci in the lowest cell, indicative of necroptosis induction. (B) NTD-DmrB cells plated on 35mm glass bottom gridded dishes and treated with 20 nM dimerizer (D) and 20 µM ZVAD-FMK. Cells were subjected to fixation, treatment with M2 (MLKL) primary antibody, and immunofluorescent RFP secondary antibody. (C) TEM immunogold labeled necroptotic cells. Immunogold particles (black foci) label the plasma membrane (red arrows, top panel), non-specific cytoplasmic contents (black arrows, top left panel), cellular remnants (lower left panel), and filamentous cellular structural components (lower right panel, blue arrows), presumably actin. (D) NTD-

DmrB cells were treated with 20 µM ZVAD-FMK. Cells were subjected to fixation and staining with M2 antibody and MLKL antibody and fluorescently labelled with fluorescent secondary antibody. M2 (red)/MLKL (green)/DAPI (blue) staining identified a discrepancy between M2 primary antibody and MLKL primary immunolabeling.

Identification of MLKL amyloid-like fibers by negative stain electron microscopy

Multiple publications have reported that oligomeric forms of MLKL are necessary for necroptosis.[2,4,5,17] Research in the Wang lab found after induction of necroptotic cell death, MLKL elutes with a size of over 2 million Da from a Superdex 200 gel filtration column, which is much larger than the previously reported tetramers (~240 kDa) and octamers (~480 kDa).[17,23] Without cell death induction, MLKL eluted as monomers (< 67kDa). In order to determine if MLKL could form a larger polymeric structure akin to the amyloid-like polymers of RIPK1/3, full length MLKL-Flag was immunoprecipitated from HeLa:GFP-RIPK3:MLKL-Flag cells undergoing necroptotic cell death (Fig. 2.2A, left panel).[21] MLKL polymers from the eluate MLKL were identified on SDD-AGE gel (Fig. 2.2A, right panel). Incubation of the eluate with 10mm of DTT for 30 minutes dissociated the MLKL polymers, establishing structural dependence on disulfide bonds.[23] To exclude the contribution of other proteins in the whole cell lysate to polymer formation, these findings were recapitulated *in vitro*. Recombinant NTD-MLKL-Flag (generated by Eduardo Reynoso) formed a polymer stable in 2% SDS following incubation at room temperature (Fig. 2.2B). The NTD-MLKL eluate from whole cell lysates and the recombinant NTD-MLKL protein were

subjected to negative staining and electron microscopy. Fibrillar forms were identified in both samples (Fig. 2.2C). The fibers obtained from cells had a consistent diameter (5.1 nm) that differed from the previously identified RIPK1/3 fibers (11-12 nm). The diameter of the recombinant protein fibers was slightly smaller (4.6 nm) than those isolated from cells. This difference was attributed to the absence of the C-terminus pseudokinase domain in the recombinant MLKL protein.

A

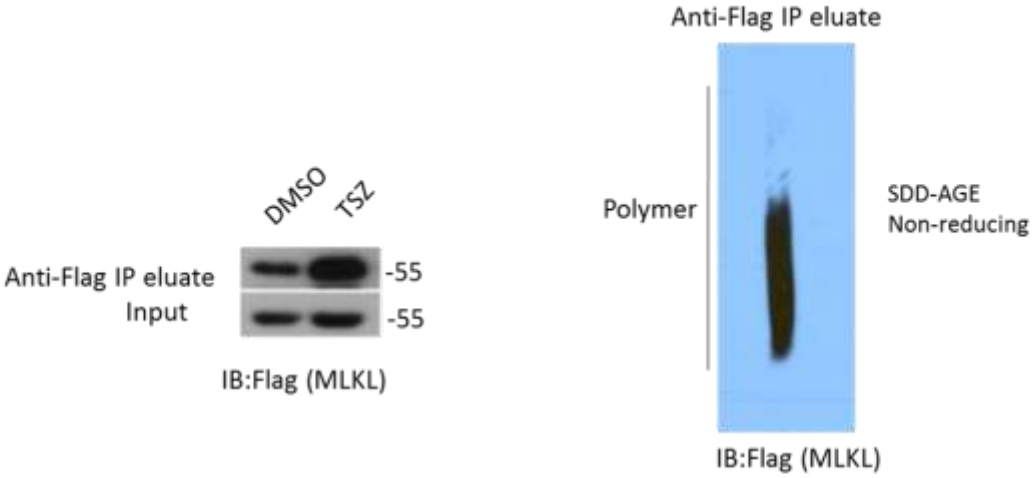

B

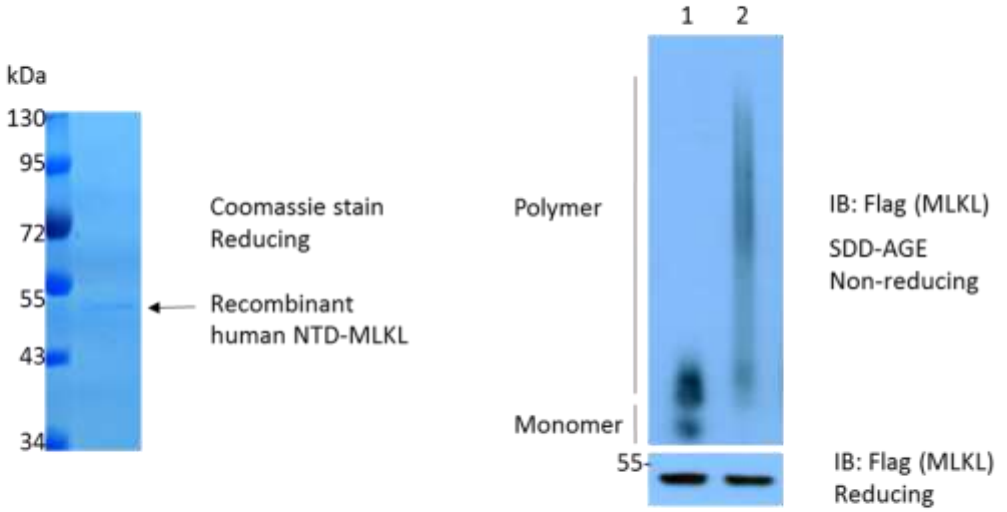

1. NTD-MLKL: no incubation
2. NTD-MLKL: incubated at 25°C, 3 hours

C

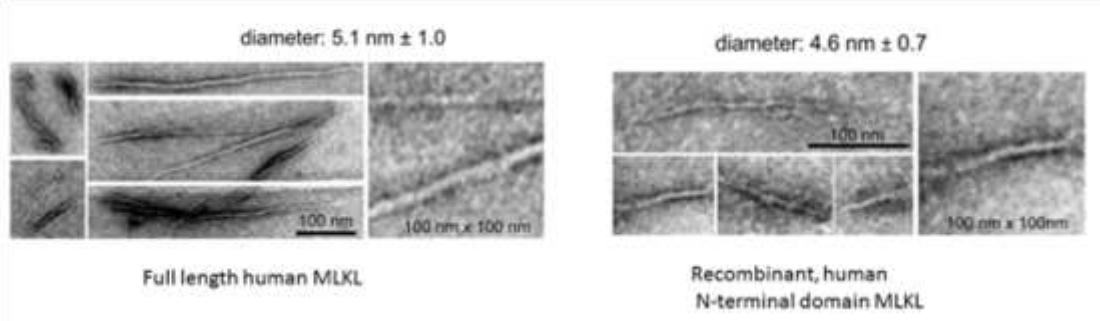

Figure 2.2. Negative stain electron microscopy of MLKL fibers
(A, left panel) Cell lysates were subjected to immunoprecipitation (IP) with anti-Flag beads, eluted with pH3 buffer, and analyzed by Western blotting. (Right panel) Eluate from immunoprecipitation of the TSZ treated lysates was analyzed by SDD-AGE. (B, left panel) Recombinant NTD-MLKL (200nM) protein was analyzed by reducing SDS-PAGE and stained with Coomassie Blue Dye. (Right panel) Recombinant NTD-MLKL protein was incubated at 25°C for 0 hr or 3 hr. Total 50 ng protein was loaded for SDD-AGE. Total 50 ng of purified GST-NTD-MLKL protein was analyzed by reducing SDS-PAGE. (C, left panel) Eluate from immunoprecipitation of the TSZ treated lysates was subjected to negative staining and analyzed by electron microscope (EM). Bar represents 100 nm. At least 10 fibers were measured to calculate the average diameter. (Right panel) Recombinant NTD polymers were subjected to negative staining and analyzed by EM. Bar represents 100 nm. At least 10 fibers were measured to calculate the average diameter.*Figures 2.2A and C have been published previously.[23]

Discussion

Subcellular localization

The immunogold results are inconclusive for determining MLKL necroptotic subcellular localization. The greatest confounding factor was the lack of M2 antibody specificity, realized after the third immunogold experiment. Ideally, direct MLKL antibody labelling should have been undertaken. This was not originally pursued due to concerns about the low intensity of direct MLKL immunofluorescence staining

using confocal microscopy. Further, measurement of endogenous MLKL would avoid potential atypical subcellular localization due to overexpression. Given the diversity of phosphoinositides targeted by MLKL *in vitro*, further investigation and refinement of the immunofluorescent/immunogold labeling may be worthwhile.

MLKL: gain-of-function polymer

Evolutionarily conserved, prion-like signaling proteins or protein complexes such as mitochondrial antiviral signaling protein (MAVS) and the apoptosis associated spec-like protein (ASC), differ from other prion-like proteins in that they are gain-of-function polymers and their conformation is key to their function.[24,25] The identification of an MLKL amyloid-like fiber distinct from the RIPK1-RIPK3 amyloid-like signaling complex, makes it the second prion-like structure identified in the necroptosis signaling pathway.[21-23] Based on biochemical evidence, generation of the polymeric form of MLKL is a required step in the necroptotic pathway, suggesting that it too is a gain-of-function polymer. Similarities between the amyloid-like MLKL polymer and the MAVS and ASC signalosomes set them apart from other typical prion domains. For example, their monomeric forms are not enriched in glutamine and asparagine and the monomers undergo regulated prion conversion.[25,26] In contrast to MAVS and ASC signalosomes, but similar to the RIPK1-RIPK3 filament, MLKL polymers stain with Congo Red that binds to β-pleated sheet conformations, suggesting that the α helical structure of the N-terminus of MLKL is not conserved in the polymeric form, although this remains to be determined.[22,23] It is relevant to note that the fibers do not stain with thioflavin and this is atypical to β amyloids. Further,

MLKL oligomerization and membrane translocation requires the chaperone HSP90 and its co-chaperone Cdc37.[27,28] Although the heat shock proteins are widely associated with prion templating, chaperones do not appear to be required for MAVS or ASC polymer assembly.

The exact function of the MLKL polymer is still unclear. The homology between the 4HB of MLKL and the N-terminus HeLo-like domain (HELL) of the fungal protein HELLP identified by Daskalov *et al.* may be relevant.[29] The HELL domain functions analogously to the HET-S protein from the ascomycete fungus *Podospora anserine,* which permeabilizes plasma membranes through an N-terminus α-helical globular, pore-forming domain (HeLo).[26,29,30] The HET-S/s C-terminus prion domain is required for amyloid propagation. In prion form, the C-terminus of HET-s adopts a β solenoid fold which transconforms the HET-S prion domain during cell fusion. This leads to refolding of the HET-S HeLo domain exposing a helix capable of permeating the membrane and propagating peripheral cellular migration leading to cell death via pore formation.[29] HET-S does not form a prion.[31,32] The HeLo domain of Het-s, which differs from the HET-S HeLo domain by 13 residues, is non-toxic.[30] This raises the question: Which MLKL molecular species causes membrane disruption? Is the MLKL polymer a toxic amyloid–like fibril or could it serve an alternative purpose as a seed for a toxic MLKL monomer or oligomer. Alternatively, MLKL may not be directly involved in structure dysfunction, it could serve as an intracellular signalosome or locally transmissible prion-like protein within an extracellular vesicle pathway.[33]

Could PolyQ proteins and MLKL share a similar mechanism of cytotoxicity?

Another potentially applicable model for MLKL induced cell damage and dysfunction are the polyglutamine (PolyQ) fibrils associated with multiple degenerative diseases (huntingtin in Huntington's disease, α-synuclein in Parkinson's disease, β-amyloid in Alzheimer's disease). The polyQ stretches shared by these aggregate prone proteins are causal to misfolding and correlated to severity of disease.[34, 35] Amyloidogenic protein misfolding leads to nucleation-dependent generation of polymorphic oligomers and fibrils. Oligomeric aggregates, composed of a small numbers of molecules and large numbers of non-filamentous assemblies, are believed to be the toxic species.[36,37] Exposure to oligomers disrupts giant unilamellar vesicle membranes through shifts in bilayer rigidity and adhesion force, inducing leakage of intravesicular contents.[37] Yet, the fibrils may also contribute to membrane damage as in the case of type 2 diabetes mellitus. [36,38-40] Human islet amyloid polypeptide (hIAPP) fibril growth at the extravesicular membrane of large unilamellar vesicles causes breakdown of cell barrier function. *In vitro*, the rate of leakage is accelerated by the presence of preformed seeds suggesting that fibril elongation rather than intermediate oligomers are the cause of the membrane damage. Fibrils can extract lipid at the liposome contact point of distortion.[40] *In vivo,* this is followed by intracellular calcium dysregulation and oxidative stress.[39,41]

Although MLKL lacks polyQ tracts, the polymeric expansion may represent a common mechanism for membrane breakdown in that both cellular damage

scenarios require intimate association of negatively charged membrane lipids and positively charged residues or areas of high positive charge density on the protein polymer.

Conclusions

Research in the field of necroptosis and other programmed cell death pathways has grown exponentially in the past decade. Despite the vast accumulation of data, the intricacies and inter-relatedness of necroptosis and other regulated cell death pathways hinder therapeutic application to the treatment of human disease. The discovery of a polymeric MLKL fiber is an intriguing addition to the pool of prion-like protein effectors in inflammatory signaling, but it does not answer the key mechanistic question of how plasma membrane disruption occurs. Rather, it encourages further exploration of the complexities of the cell death pathways.

References

1. Petrie, E.J., Hildebrand, J.M. & Murphy, J.M. Insane in the membrane: a structural perspective of MLKL function in necroptosis. *Immunol Cell Biol* **95**, 152-159 (2017).
2. Su, L.*, et al.* A plug release mechanism for membrane permeation by MLKL. *Structure* **22**, 1489-1500 (2014).
3. Wang, H.*, et al.* Mixed lineage kinase domain-like protein MLKL causes necrotic membrane disruption upon phosphorylation by RIP3. *Mol Cell* **54**, 133-146 (2014).
4. Cai, Z.*, et al.* Plasma membrane translocation of trimerized MLKL protein is required for TNF-induced necroptosis. *Nat Cell Biol* **16**, 55-65 (2014).
5. Dondelinger, Y.*, et al.* MLKL compromises plasma membrane integrity by binding to phosphatidylinositol phosphates. *Cell Rep* **7**, 971-981 (2014).
6. Chen, X.*, et al.* Translocation of mixed lineage kinase domain-like protein to plasma membrane leads to necrotic cell death. *Cell Res* **24**, 105-121 (2014).
7. Tanzer, M.C.*, et al.* Evolutionary divergence of the necroptosis effector MLKL. *Cell Death Differ* **23**, 1185-1197 (2016).

8. Falkenburger, B.H., Jensen, J.B., Dickson, E.J., Suh, B.C. & Hille, B. Phosphoinositides: lipid regulators of membrane proteins. *J Physiol* **588**, 3179-3185 (2010).
9. Wang, Z., Jiang, H., Chen, S., Du, F. & Wang, X. The mitochondrial phosphatase PGAM5 functions at the convergence point of multiple necrotic death pathways. *Cell* **148**, 228-243 (2012).
10. Murphy, J.M.*, et al.* The pseudokinase MLKL mediates necroptosis via a molecular switch mechanism. *Immunity* **39**, 443-453 (2013).
11. Remijsen, Q.*, et al.* Depletion of RIPK3 or MLKL blocks TNF-driven necroptosis and switches towards a delayed RIPK1 kinase-dependent apoptosis. *Cell Death Dis* **5**, e1004 (2014).
12. Tait, S.W.*, et al.* Widespread mitochondrial depletion via mitophagy does not compromise necroptosis. *Cell Rep* **5**, 878-885 (2013).
13. Galluzzi, L.*, et al.* Molecular mechanisms of cell death: recommendations of the Nomenclature Committee on Cell Death 2018. *Cell Death Differ* **25**, 486-541 (2018).
14. Tanzer, M.C.*, et al.* Necroptosis signalling is tuned by phosphorylation of MLKL residues outside the pseudokinase domain activation loop. *Biochem J* **471**, 255-265 (2015).
15. Hildebrand, J.M.*, et al.* Activation of the pseudokinase MLKL unleashes the four-helix bundle domain to induce membrane localization and necroptotic cell death. *Proc Natl Acad Sci U S A* **111**, 15072-15077 (2014).
16. Quarato, G.*, et al.* Sequential Engagement of Distinct MLKL Phosphatidylinositol-Binding Sites Executes Necroptosis. *Mol Cell* **61**, 589-601 (2016).
17. Huang, D.*, et al.* The MLKL Channel in Necroptosis Is an Octamer Formed by Tetramers in a Dyadic Process. *Mol Cell Biol* **37**(2017).
18. Xia, B.*, et al.* MLKL forms cation channels. *Cell Res* **26**, 517-528 (2016).
19. Zhang, Y., Chen, X., Gueydan, C. & Han, J. Plasma membrane changes during programmed cell deaths. *Cell Res* (2017).
20. Gong, Y.N.*, et al.* ESCRT-III Acts Downstream of MLKL to Regulate Necroptotic Cell Death and Its Consequences. *Cell* **169**, 286-300 e216 (2017).
21. Mompean, M.*, et al.* The Structure of the Necrosome RIPK1-RIPK3 Core, a Human Hetero-Amyloid Signaling Complex. *Cell* (2018).
22. Li, J.*, et al.* The RIP1/RIP3 necrosome forms a functional amyloid signaling complex required for programmed necrosis. *Cell* **150**, 339-350 (2012).
23. Liu, S.*, et al.* MLKL forms disulfide bond-dependent amyloid-like polymers to induce necroptosis. *Proc Natl Acad Sci U S A* (2017).
24. Liu, S.*, et al.* MAVS recruits multiple ubiquitin E3 ligases to activate antiviral signaling cascades. *Elife* **2**, e00785 (2013).
25. Cai, X., Xu, H. & Chen, Z.J. Prion-Like Polymerization in Immunity and Inflammation. *Cold Spring Harb Perspect Biol* **9**(2017).

26. Cai, X.*, et al.* Prion-like polymerization underlies signal transduction in antiviral immune defense and inflammasome activation. *Cell* **156**, 1207-1222 (2014).
27. Zhao, X.M.*, et al.* Hsp90 modulates the stability of MLKL and is required for TNF-induced necroptosis. *Cell Death Dis* **7**, e2089 (2016).
28. Jacobsen, A.V.*, et al.* HSP90 activity is required for MLKL oligomerisation and membrane translocation and the induction of necroptotic cell death. *Cell Death Dis* **7**, e2051 (2016).
29. Daskalov, A.*, et al.* Identification of a novel cell death-inducing domain reveals that fungal amyloid-controlled programmed cell death is related to necroptosis. *Proc Natl Acad Sci U S A* **113**, 2720-2725 (2016).
30. Saupe, S.J. & Daskalov, A. The [Het-s] prion, an amyloid fold as a cell death activation trigger. *PLoS Pathog* **8**, e1002687 (2012).
31. Loquet, A. & Saupe, S.J. Diversity of Amyloid Motifs in NLR Signaling in Fungi. *Biomolecules* **7**(2017).
32. Greenwald, J.*, et al.* The mechanism of prion inhibition by HET-S. *Mol Cell* **38**, 889-899 (2010).
33. Eisenberg, D. & Jucker, M. The amyloid state of proteins in human diseases. *Cell* **148**, 1188-1203 (2012).
34. Zoghbi, H.Y. & Orr, H.T. Glutamine repeats and neurodegeneration. *Annu Rev Neurosci* **23**, 217-247 (2000).
35. Scarafone, N.*, et al.* Amyloid-like fibril formation by polyQ proteins: a critical balance between the polyQ length and the constraints imposed by the host protein. *PLoS One* **7**, e31253 (2012).
36. Relini, A., Marano, N. & Gliozzi, A. Misfolding of amyloidogenic proteins and their interactions with membranes. *Biomolecules* **4**, 20-55 (2013).
37. Ho, C.S., Khadka, N.K., She, F., Cai, J. & Pan, J. Polyglutamine aggregates impair lipid membrane integrity and enhance lipid membrane rigidity. *Biochim Biophys Acta* **1858**, 661-670 (2016).
38. Relini, A., Marano, N. & Gliozzi, A. Probing the interplay between amyloidogenic proteins and membranes using lipid monolayers and bilayers. *Adv Colloid Interface Sci* **207**, 81-92 (2014).
39. Engel, M.F.*, et al.* Membrane damage by human islet amyloid polypeptide through fibril growth at the membrane. *Proc Natl Acad Sci U S A* **105**, 6033-6038 (2008).
40. Milanesi, L.*, et al.* Direct three-dimensional visualization of membrane disruption by amyloid fibrils. *Proc Natl Acad Sci U S A* **109**, 20455-20460 (2012).
41. Pieri, L., Madiona, K., Bousset, L. & Melki, R. Fibrillar alpha-synuclein and huntingtin exon 1 assemblies are toxic to the cells. *Biophys J* **102**, 2894-2905 (2012).
42. Halfmann, R. & Lindquist, S. Screening for amyloid aggregation by Semi-Denaturing Detergent-Agarose Gel Electrophoresis. *J Vis Exp* (2008).

CHAPTER THREE
Necroptosis blocking compound 1 (NBC1) inhibits necroptosis by conjugating Hsp70 and abrogating MLKL polymerization

Introduction

The recognition of small-molecules that block necroptosis such as the RIPK1 inhibitor necrostatin (Nec-1), the MLKL inhibitor necrosulfonamide (NSA), and 17AAG the heat shock protein 90 (Hsp90) antagonist were key in understanding the core-signaling pathway and the discovery of ancillary proteins like Hsp90, which facilitates the final stages of necroptosis.[1-6] Hsp90 is an abundant and highly conserved molecular chaperone with a diverse set of client proteins, many of which are members of the kinome. Interactions are dependent on recognition of the kinase or pseudokinase domain by co-chaperone CDC37.[4,6,7] Hsp90 interacts with RIPK1, RIPK3, and MLKL, affecting protein stability and function. Inhibition of Hsp90 prevents RIPK1 interaction with RIPK3 and blocks phosphorylation of RIPK3 and MLKL, abrogating necroptosis.[3,7] Hsp90 promotes MLKL oligomerization and plasma membrane translocation; however, Hsp90 inhibitors are unable to block necroptosis in cells over-expressing N-terminus MLKL (residues 1-180) death effector domain, the 4HB.[4] Through an unbiased small molecule screen, we have identified a novel chemical inhibitor of necroptosis that targets an additional molecular chaperone, heat shock protein 70 (Hsp70). As with Hsp90, Hsp70 stabilizes MLKL and promotes MLKL polymerization, but unlike Hsp90, Hsp70 interacts with the N-terminus domain

of MLKL. This work expands the role of heat shock proteins in necroptosis.

Results

Identification of a novel necroptosis blocking compound (NBC1)

We performed a forward small molecule screen using libraries provided by The National Cancer Institute's Developmental Therapeutics Program Open Chemical Repository to identify inhibitors of TNFα induced necroptosis. Using a phenotypic cell death assay, 2,675 small molecules were evaluated. We initiated the screen with the colon cancer cell-line, HT-29, which undergoes TNFα mediated necroptosis using conventional stimuli: TNFα (T) to activate TNFR1, Smac mimetic (S) to inhibit cIAP-mediated ubiquitylation of RIPK1, and ZVAD-FMK (Z), the pan-caspase inhibitor to inhibit caspase 8.[2,8] Necroptosis inhibitors of RIPK1 (Necrostatin) and MLKL (Necrosulfonamide, NSA) were used as positive controls.[2,9] Successful candidate compounds from the first tier were tested in NTD-DmrB HeLa cells, which stably express a truncated MLKL transgene containing the N-terminus domain (NTD: 1-190 amino acids), or death effector domain, fused to a chemically-inducible, dimerizable (DmrB) domain driven by a Tet-inducible promoter. Use of NTD-DmrB cells bypassed the proximal necroptosis signaling cascade and identified inhibitors that acted downstream of MLKL dimerization. A third tier assay used mouse fibroblast L929 cells. Because cysteine 86 targeted by NSA is not conserved in the *Mus musculus* MLKL homolog, NSA is ineffective in murine cells, ensuring

that any novel MLKL inhibitors would have a mechanism unique from NSA. From the tiered screen, a single small molecule, Necroptosis Blocking Compound-1 (NBC1), effectively blocked necroptosis in all cell lines (Fig. 3.1A-D). NBC1 had variable EC_{50} values in HT-29 (0.5µM), NTD-DmrB (2.9µM), and L929 cells (7.5µM) which may reflect inherent cell type and species differences.

NBC1 was further analyzed to determine compond stabililty and aidentify active structural characteristic. The metabolic S9 stability assay of NBC1 found that the compound has a predicted half-life of 1.1 minutes, limiting its use to cell culture systems. NBC1 analogs were generated to perform structure activity relationship studies (SAR) (Fig. 3.1E, F). Compound activity correlated with higher numbers of α,β-unsaturated enone moieties, presumably acting as Michael acceptors, which suggests that this functional group is required for NBC1's biological activity.

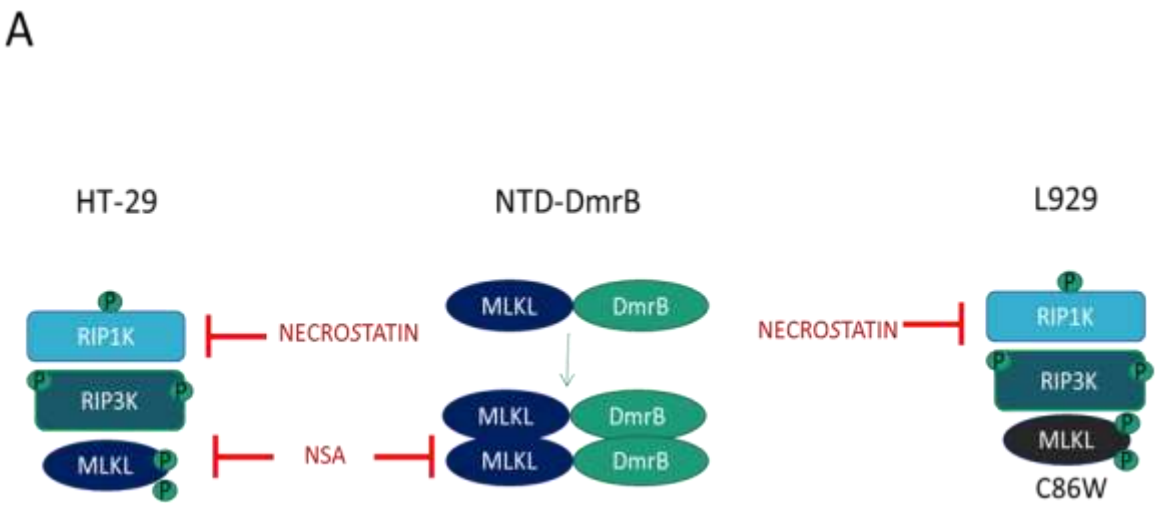

B

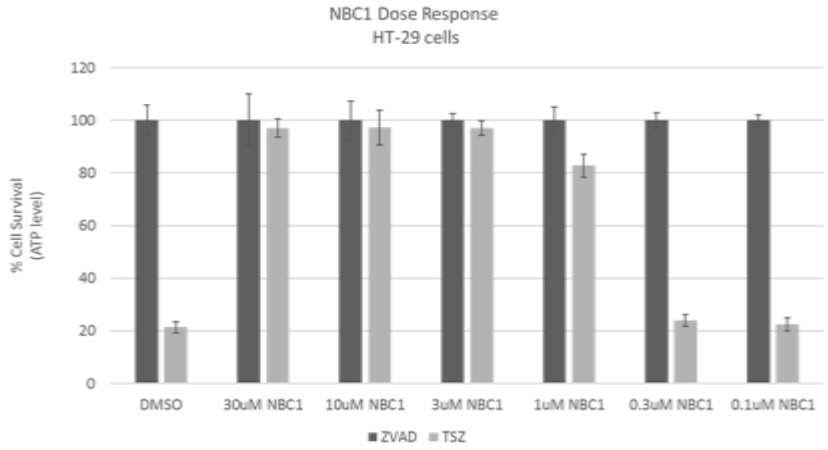
NBC1 Dose Response
HT-29 cells
% Cell Survival
(ATP level)
120
100
80
60
40
20
0
DMSO
30uM NBC1
10uM NBC1
3uM NBC1
1uM NBC1
0.3uM NBC1
0.1uM NBC1
ZVAD
TSZ

C

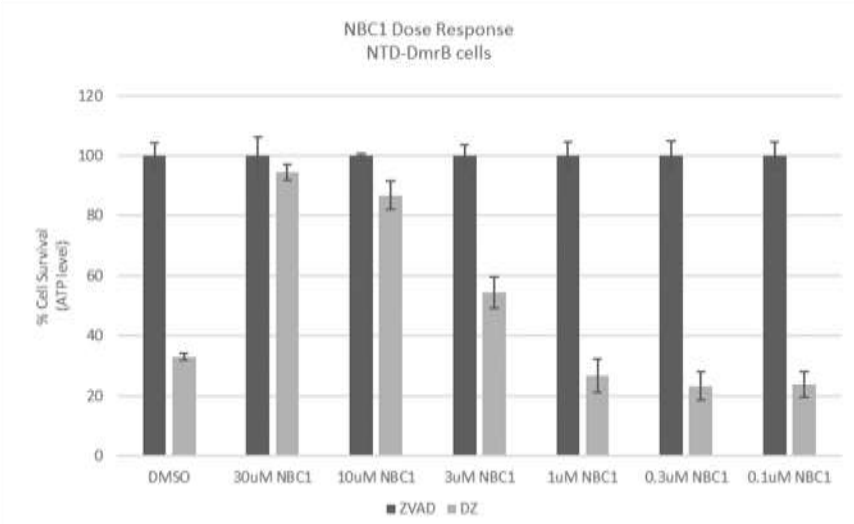
NBC1 Dose Response
NTD-DmrB cells
% Cell Survival
(ATP level)
120
100
80
60
40
20
0
DMSO
30uM NBC1
10uM NBC1
3uM NBC1
1uM NBC1
0.3uM NBC1
0.1uM NBC1
ZVAD
DZ

D

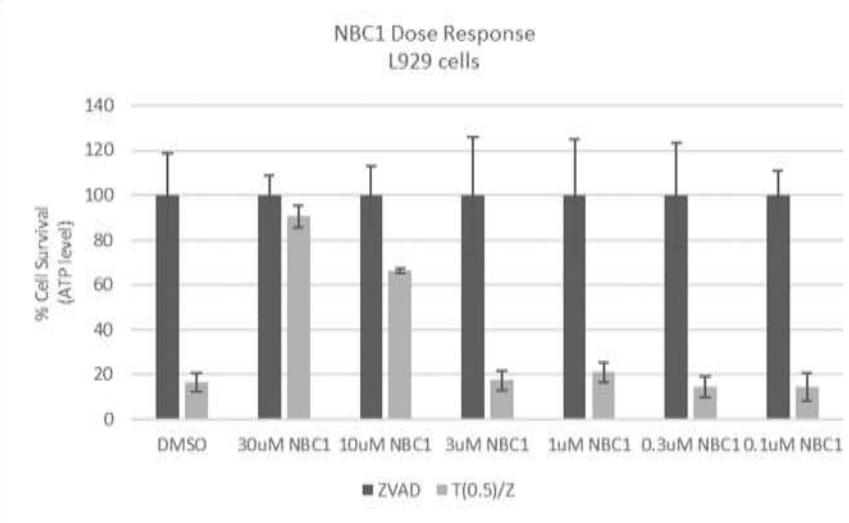
NBC1 Dose Response
L929 cells
% Cell Survival (ATP level)
140
120
100
80
60
40
20
0
DMSO
30uM NBC1
10uM NBC1
3uM NBC1
1uM NBC1
0.3uM NBC1
0.1uM NBC1
ZVAD
T(0.5)/Z

E

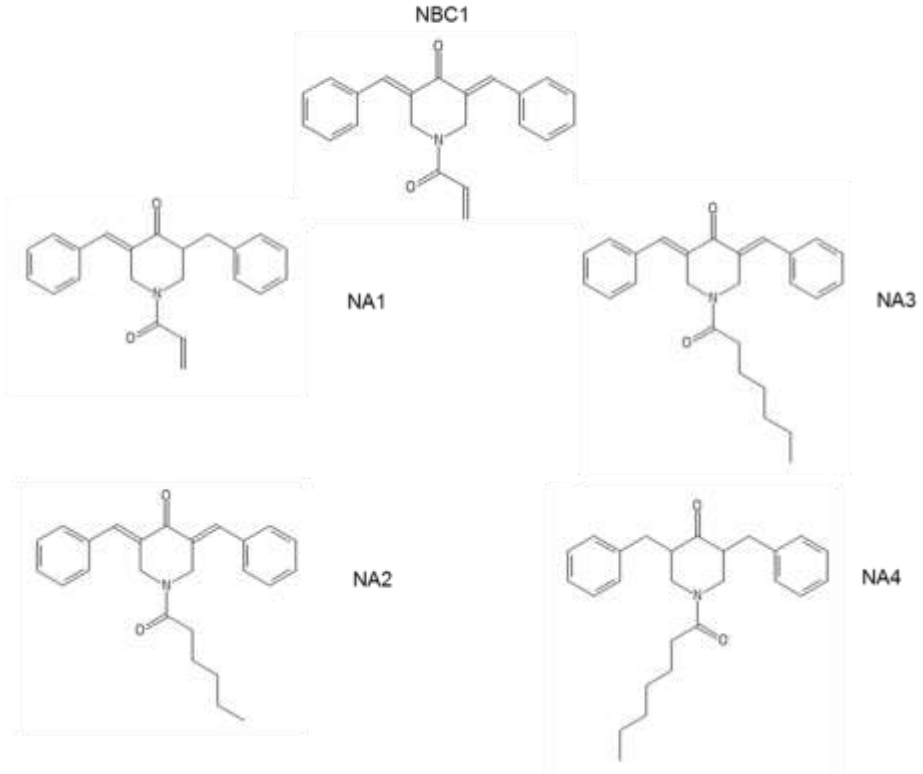
NBC1
NA1
NA3
NA2
NA4

F

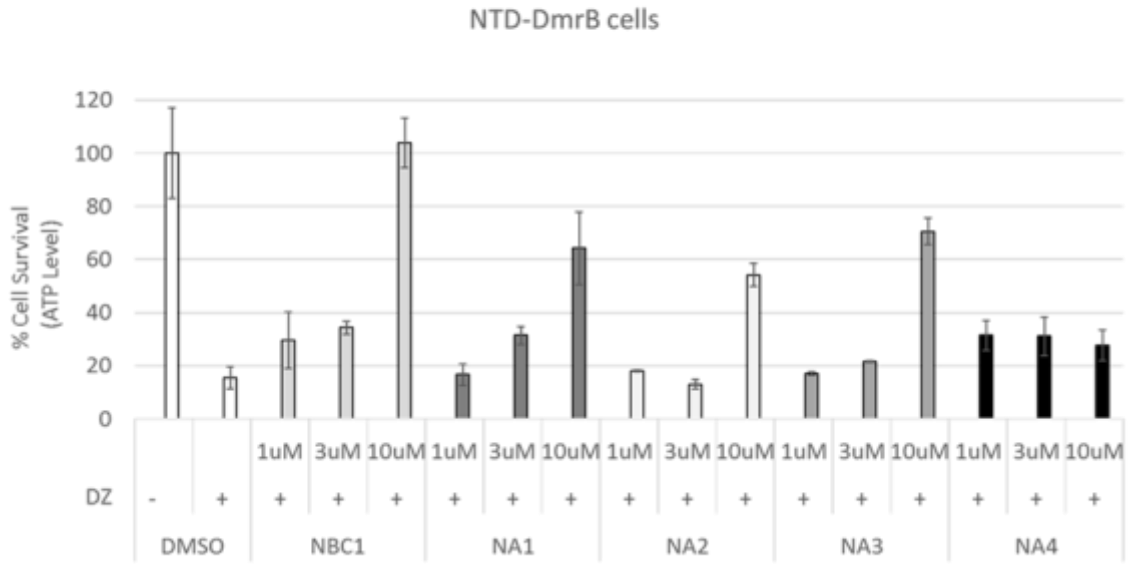

Figure 3.1. Identification of novel necroptosis blocking compound (NBC1) from NCI Open Chemical Repository Collection.
(A) Tiered cell model system for forward small molecule screen. Left panel depicts the canonical necroptosis signaling cascade in HT-29 cells (tier 1), which can be blocked Necrostatin targeting RIPK1 or Necrosulfonamide (NSA) targeting MLKL. The middle panel depicts the MLKL dimerizable induction of necroptosis in HeLa MLKL knockout cells expressing the doxycycline inducible, dimerizable domain of N-terminus MLKL (NTD-DmrB, tier 2), which recapitulates the distal cell death pathway and is blocked by NSA. The right panel (tier 3) shows the mouse fibrosarcoma L929 cells.
(B) NBC1 dose-response curve in HT-29 cells. Cells were treated as indicated for 16 hours. Necroptosis was induced with TNFα (20ng/ml), Smac mimetic (100nM), and ZVAD-FMK (20μM, TSZ). Identical concentrations used in other experiments unless otherwise indicated. Cell viability was measured by the CellTiter-Glo assay. Data are represented as mean ± SD of duplicates.
(C) NBC1 dose-response curve in NTD-DmrB cells. Cells were treated as indicated for 16 hours. Necroptosis was induced with dimerizer and ZVAD-FMK (DZ). Cell survival was assessed by the CellTiter-Glo assay. Data are represented as mean ± SD of duplicates.
(D) NBC1 dose response curve in mouse fibrosarcoma L929. Cells were treated as indicated for 16 hours. Necroptosis was induced with TNF, Smac mimetic, and

ZVAD-FMK (TSZ). Cell viability was measured by the CellTiter-Glo assay. Data are represented as mean ± SD of duplicates.
(E) Chemical structures of NBC1 and its structural analogues.
(F) NTD-DmrB cells set up for NBC1 and its analogues (NBC1-A1 (NA1), NBC1-A2 (NA2), NBC1-A3 (NA3), and NBC1-A4 (NA4)) effective dose determination. Cells were treated as indicated for 16 hours. Necroptosis was induced with dimerizer and ZVAD-FMK (DZ). Cell viability was assessed by the CellTiter-Glo assay. Data are represented as mean ± SD of duplicates. NA4 identified as the negative analog (NA).

NBC1 specifically conjugates Hsp70

To aid in identification of the molecular target of NBC1, biotinylated NBC1 (B-NBC1) and negative analog (B-NA) were generated (Fig. 3.2A). The biotinylated NBC1 analog maintained its ability to block necroptosis but required a 2 fold higher concentration (Supplementary Fig. S1). Following treatment of NTD-DmrB with increasing concentrations of B-NBC1, a unique avidin positive protein was identified at approximately 72 kDa (Fig. 3.2B). B-NBC1 conjugation was competitively inhibited with non-biotinylated NBC1 but not NA (Fig. 3.2C) suggesting specific protein targeting. Mass spectroscopy identified the target as the molecular chaperone heat shock protein 70 (Hsp70). This interaction was confirmed *in vivo* using NTD-DmrB cells (Fig. 3.2D). Notably, MLKL was not identified in the mass spectroscopy analysis B-NBC1 nor did MLKL interact with B-NBC1 *in vivo*. The conjugation was found to be covalent as boiling failed to disrupt B-NBC1 binding to recombinant human Hsp70 *in vitro* (Fig 3.2E). The inverse intensity relationship between avidin-HRP and Hsp70 immunoblots in the B-NBC1 treated samples suggested blockade of the antibody-Hsp70 binding site by B-NBC1.

Heat shock protein 70 has two highly conserved domains, an N-terminus nucleotide-binding domain (NBD), which regulates the affinity of substrate binding, and a C-terminus substrate-binding domain (SBD). In order to confirm a role for Hsp70 in necroptosis, two chemical inhibitors with unique mechanisms of action were used in cell death assays (Fig. 3.2F). VER-155008 (5′-O-[(4-Cyanophenyl) methyl]-8-[[(three, 4-dichlorophenyl) methyl] amino]-adenosine), which blocks the Hsp70 NBD and acts as an ATP competitive inhibitor, did not protect NTD-DmrB cells from necroptosis.[10] Whereas PES-Cl, which binds to the SBD and disrupts interaction with client proteins, was protective.[11] This suggests that blockade of Hsp70's SBD is critical to its protective effect. To determine if NBC1 shared characteristics of other Hsp70 inhibitors, accumulation and oligomerization of p62/SQSTM1 was assessed by immunoblot following compound treatment (Fig. 3.2G).[10,11] Hsp70 inhibitors are known to disrupt autophagy and accumulation p62 oligomers mark this effect. NBC1 mimicked the action of known Hsp70 chemical inhibitors, which may have relevance as an ancillary cell death pathway.

A

Biotinylated-Necroptosis Blocking Compound-1
(B-NBC1)

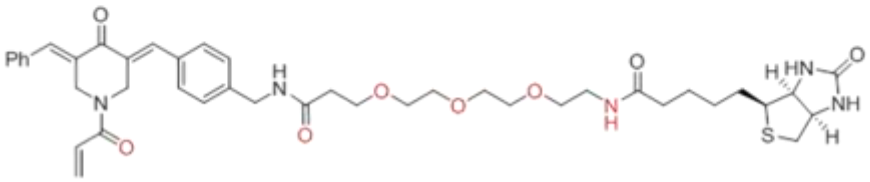

Biotinylated-Negative Analogue
(B-NA)

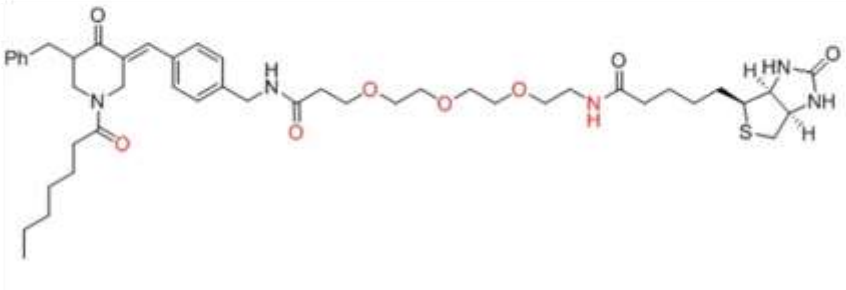

B

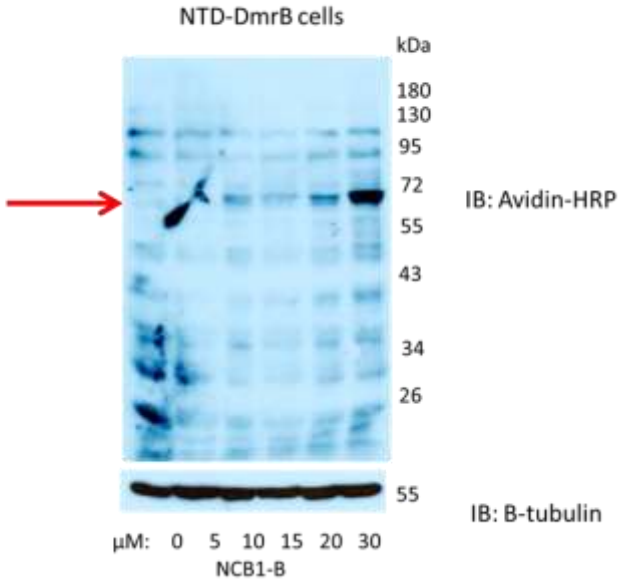
NTD-DmrB cells
kDa
180
130
95
72
55
43
34
26
IB: Avidin-HRP
55
IB: B-tubulin
µM: 0 5 10 15 20 30
NCB1-B

C

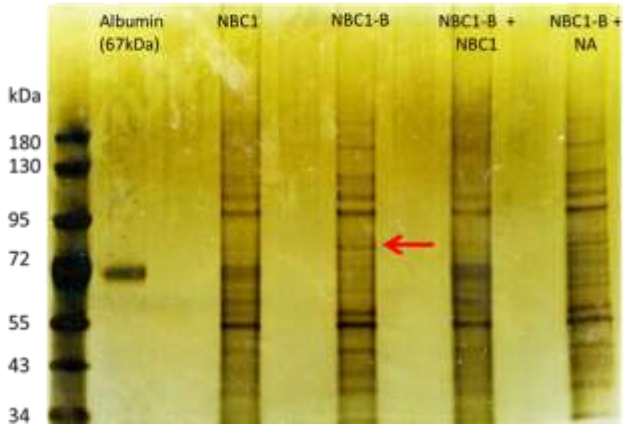
Albumin (67kDa)
NBC1
NBC1-B
NBC1-B + NBC1
NBC1-B + NA
kDa
180
130
95
72
55
43
34

D

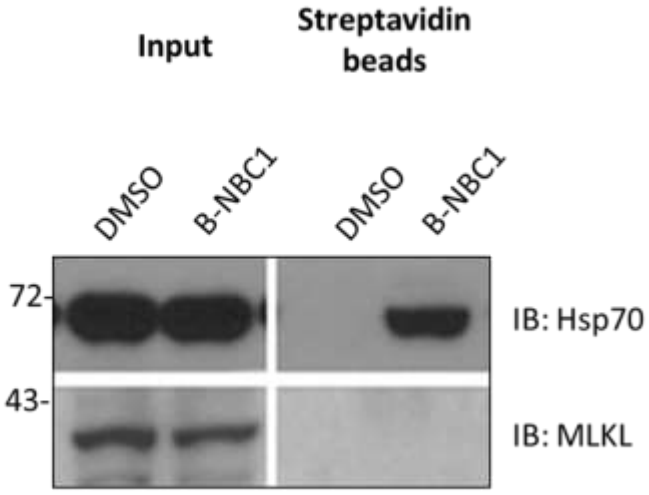
Input
Streptavidin beads
DMSO
B-NBC1
DMSO
B-NBC1
72-
43-
IB: Hsp70
IB: MLKL

E

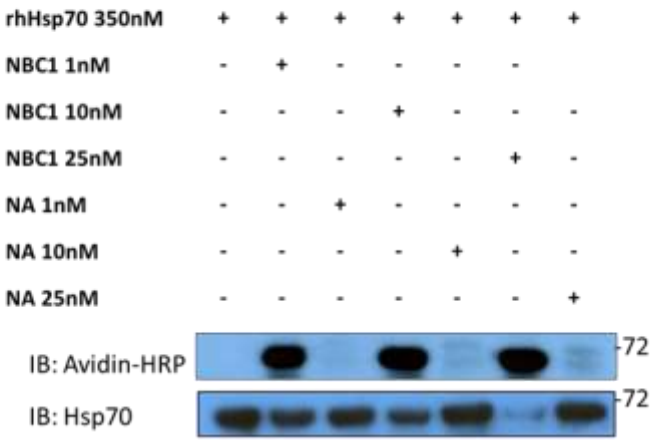
rhHsp70 350nM + + + + + + +
NBC1 1nM - + - - - -
NBC1 10nM - - - + - - -
NBC1 25nM - - - - - + -
NA 1nM - - + - - - -
NA 10nM - - - - + - -
NA 25nM - - - - - - +
IB: Avidin-HRP
IB: Hsp70
72
72

F

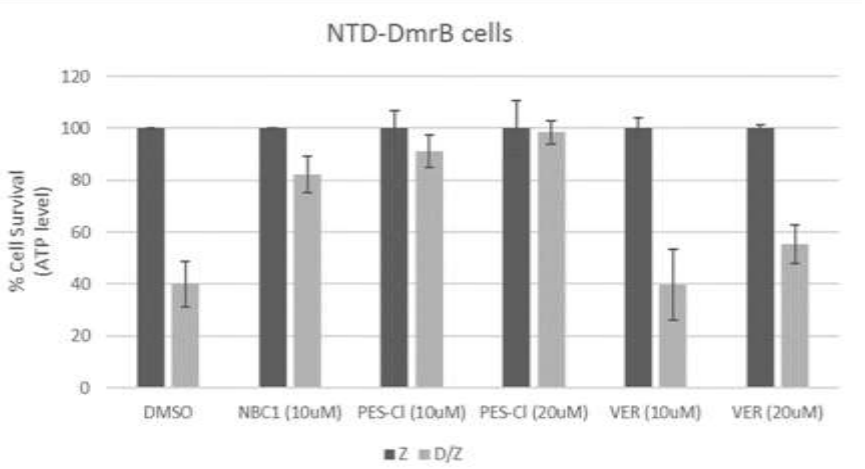

G

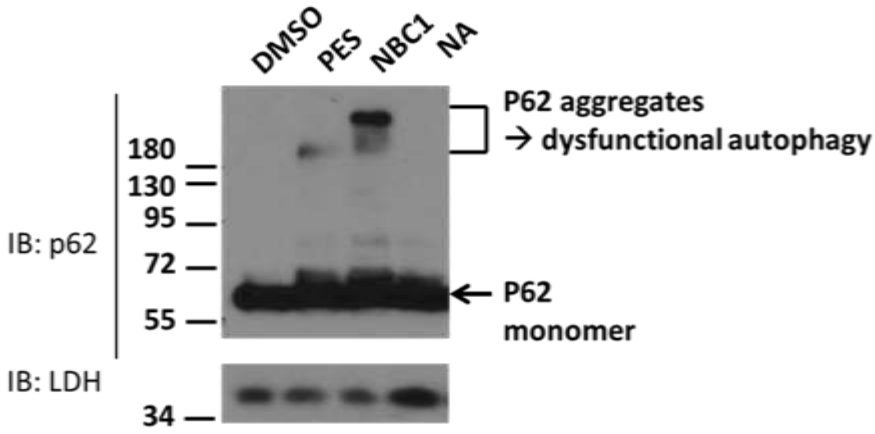

Figure 3.2. NBC1 specifically conjugates Hsp70.
(A) Chemical structures of biotinylated NBC1 (B-NBC1) and its negative analogue (B-NA).
(B) Identification of a unique avidin positive protein. NTD-DmrB cells were treated with incrementally increasing concentrations of B-NBC1. Whole cell lysates were separated by polyacrylamide gel electrophoresis followed by anti-avidin Western blot.
(C) Identification of Hsp70 as NBC1 target protein. NTD-DmrB cells were treated with biotinyated and non-biotinylated positive and negative compounds as indicated in experimental procedures describing the competitive inhibition assay. Biotin labeled proteins were precipitated with streptavidin beads. Eluates were separated by polyacrylamide gel electrophoresis and unique proteins were identified by silver

staining. Arrow identifies band excised for mass spectroscopy and identified as Hsp70.
(D) Hsp70-B-NBC1 interacts during necroptosis. Aliquots (1mg) of whole cell lysates from NTD-DmrB cells treated with DMSO or B-NBC1 were used for streptavidin precipitation. Aliquots of 20 µg whole cell lysates were subjected to Western blot to measure Hsp70 and MLKL input levels and eluate.
(E) *In vitro* conjugation assay. Recombinant human Hsp70 (rhHsp70, 350nM) treated with incrementally increasing concentrations of B-NBC1 or B-NA as indicated. Samples were boiled in SDS containing loading buffer, separated on an acrylamide gel, and subjected to Western blot with avidin-HRP and Hsp70.
(F) NTD-DmrB cells were treated as indicated for 16 hours. Cell viability was determined by measuring ATP levels. Necroptosis was induced by the addition of dimerizer and ZVAD-FMK (DZ). The data are represented as the mean ± SD of triplicate wells.
(G) NBC1 mimics P62 aggregation caused by known Hsp70 inhibitors. NTD-DmrB cells were treated with DMSO, Hsp70 inhibitor: 2-Phenylethynesulfonamide (PES, 20 µM), NBC1 (20 µM), and NA (20 µM) for 16 hours. Cell lysates were subjected to P62/SQSTM1 and LDH Western blot of P62/SQSTM1 and LDH as a loading control.

Inhibition of Hsp70 blocks MLKL polymerization

MLKL is the final protein mediator of necroptosis; therefore, we wanted to determine if Hsp70 interacted directly with MLKL. Immunoprecipitation of Flag-tagged MLKL from the NTD-DmrB cells pulled-down endogenous Hsp70 in cells undergoing necroptosis but not under control conditions (Fig. 3.3A). The Hsp70 pull-down was not inhibited by NSA suggesting that although cell death had been prevented the interaction between MLKL and the stress-inducible Hsp70 persists. Inhibitors of Hsp90 destabilize core necroptotic mediators and reduce MLKL phosphorylation and polymerization, we wanted to determine if Hsp70 had a similar mechanism of action. RIPK1, RIPK3, and MLKL expression is stable in HT-29 cells treated with NBC1 for 16 hours. Unlike chemical inhibition of Hsp90, phosphorylation of MLKL was also unaffected by treatment with NBC1, indicating

that NBC1's protective effect occurs downstream (Fig. 3.3B). NBC1 did not inhibit tetramer formation NTD-DmrB or HT-29 cell (Fig. 3.3C and D). To determine if Hsp70 could affect polymerization of MLKL, a Semi-Denaturing Detergent Agarose Gel Electrophoresis was employed.[12] This is a method for detecting and characterizing large protein polymers, which are stable in 2% SDS at room temperature, unlike most large protein complexes. In HT-29 and NTD-DmrB cells treated with DMSO or NA, the polymeric form of MLKL is visible, whereas, treatment with NBC1 inhibits MLKL polymerization similar to NSA (Fig. 3.3E and F).[9,13]

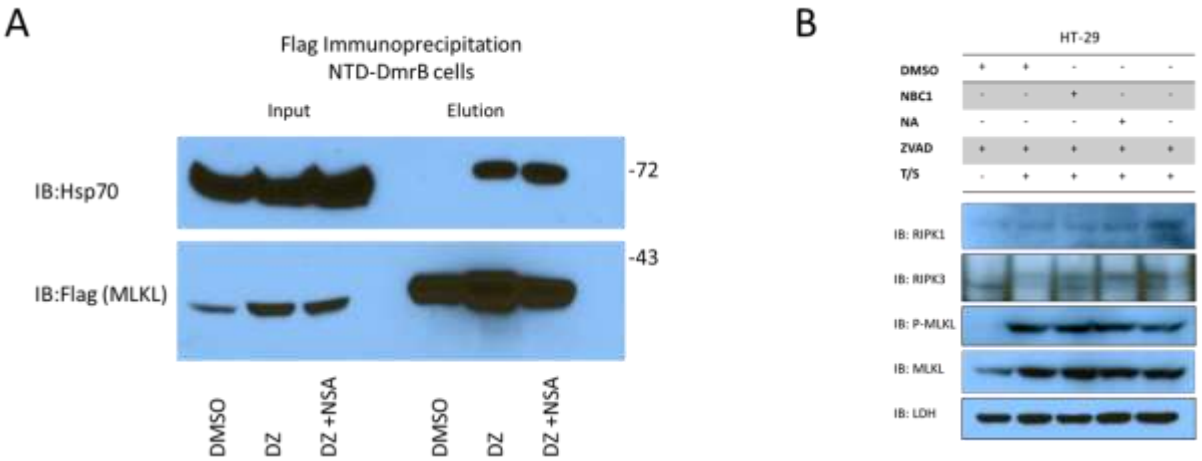

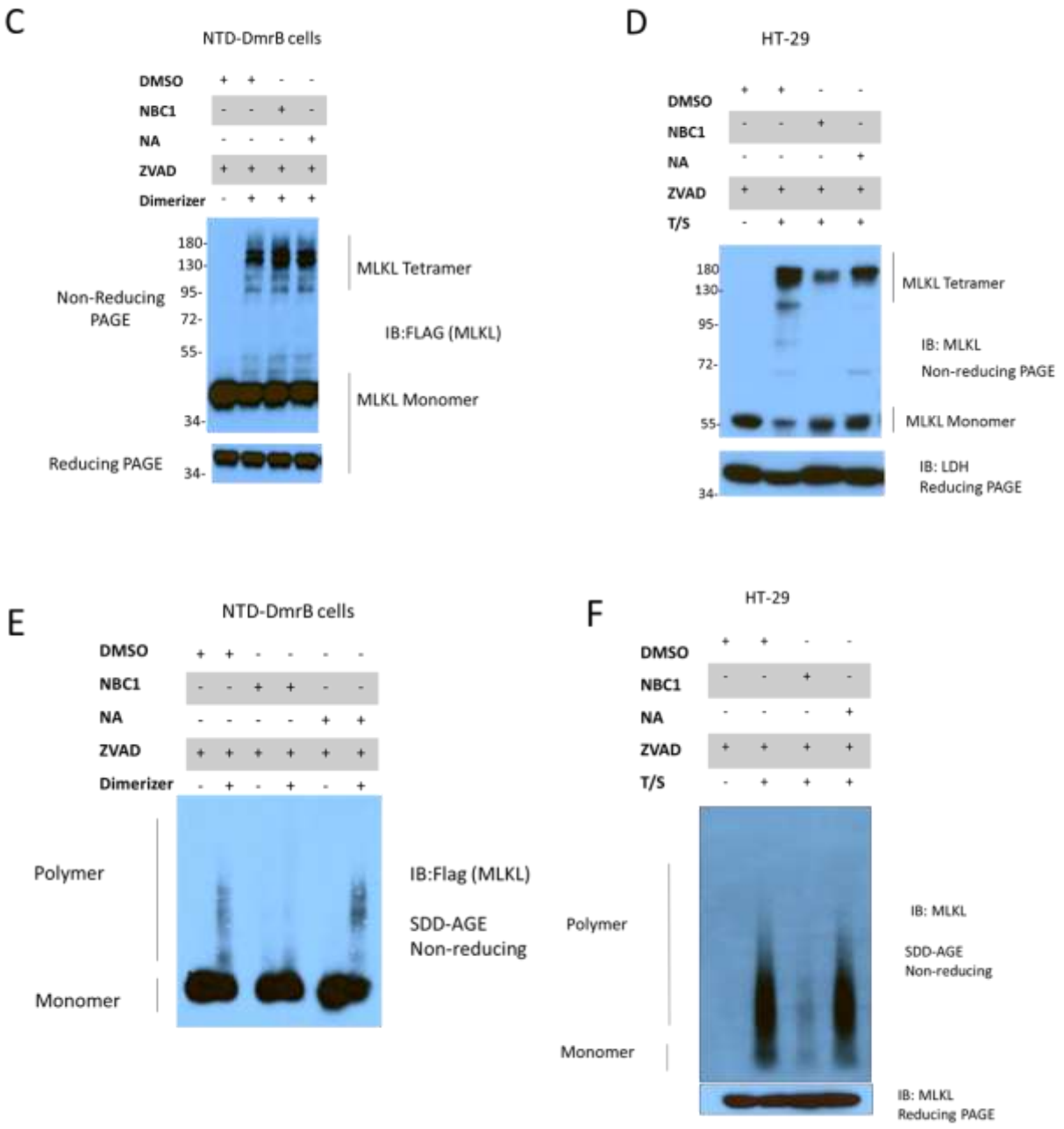

Figure 3.3. Chemical inhibition of Hsp70 C-terminus substrate binding domain blocks necroptosis

(A) Hsp70 co-immunoprecipitated with MLKL during necroptosis. NTD-DmrB cells were treated as indicated. Flag-tagged MLKL was immunoprecipitated with anti-Flag antibody from cell lysates. Western blotting using antibodies as indicated analyzed immunocomplexes.

(B) The effects of NBC1 on the necroptosis protein mediators. HT-29 cells were treated with DMSO, NBC1 (10 µM), or NA (10 µM) for 16 hours. Necroptosis was induced with TSZ. Whole cell lysates were separated by SDS-PAGE and subjected to Western blot with RIPK1, RIPK3, Phospho-MLKL, MLKL, and LDH as a loading control. The subtle double band in the TSZ treated sample in the RIPK3 immunoblot is suggestive of phosphorylation. Phosphorylation of MLKL which occurs downstream of necrosome formation is positive in the TSZ treated samples.
(C) NBC1 does not modify MLKL tetramer formation in NTD-DmrB cells. Cells were treated with DMSO, NBC1 (10 µM), or NA (10 µM) for 16 hours. Necroptosis was induced with DZ. Whole cell lysates were separated by non-reducing and reducing SDS-PAGE and subjected to Western blot analysis with the antibodies indicated.
(D) NBC1 does not modify MLKL tetramer formation in HT-29 cells. Cells were treated with DMSO, NBC1 (10 µM), or NA (10 µM) for 16 hours. Necroptosis was induced with DZ. Whole cell lysates were separated by non-reducing and reducing SDS-PAGE and subjected to Western blot analysis with the antibodies indicated.
(E) NBC1 blocks MLKL polymerization in NTD-DmrB cells. Cells were treated with DMSO, NBC1 (10 µM), or NA (10 µM) for 16 hours. Necroptosis was induced with DZ. Whole cell lysates were subjected to Semi-Denaturing Detergent Agarose Gel Electrophoresis (SDD-AGE), reducing SDS-PAGE, and immunoblot with M2-HRP to assess MLKL polymerization.
(F) NBC1 blocks MLKL polymerization in HT-29 cells. Cells were treated with DMSO, NBC1 (10 µM), or NA (10 µM) for 16 hours. Necroptosis was induced with DZ. Whole cell lysates were subjected to SDD-AGE, reducing SDS-PAGE, and immunoblot with MLKL to assess polymerization.

Hsp70 promotes MLKL polymerization in vitro

Hsp70 and, highly homologous heat shock cognate 70 (Hsc70), enhance polymerization of recombinant N-terminus domain-GST-MLKL-FLAG (rhMLKL; Fig. 3.4A). Treatment of rhMLKL with NBC1 attenuates the generation of the amyloid–like polymer relative to treatment with NA (Fig. 3.4B). Recombinant N-terminus NBD (residue 2-385) and C-terminus SBD (residue 390-616) Hsp70 truncation proteins were generated to determine which region promoted polymerization (Fig 3.4C). MLKL polymerization was abrogated by recombinant NBD Hsp70 and enhanced with recombinant SBD Hsp70 compared to full length Hsp70 (Fig 3.4D). The

substrate-binding domain (SBD) of Hsp70 is divided into ß-sheet and α-helical lid subdomains. Recalling the SAR studies, we hypothesized that the robustly nucleophilic cysteines within the α-helical lid subdomain, the only cysteines in the C-terminus, may be NBC1's target amino acids. The cysteine residues were mutated to serines (C574S, C603S, C574/603S). Single and double cysteine mutagenesis abrogated the NBC1 binding affinity for the SBD of Hsp70 (Fig. 3.4E). Further, the mutagenized C-terminus Hsp70 proteins (C574S, C603S) diminished the polymerization of MLKL as compared to full length and C-terminus recombinant Hsp70 and the effect was additive in the double mutant (C574/603S; Fig. 3.4F).

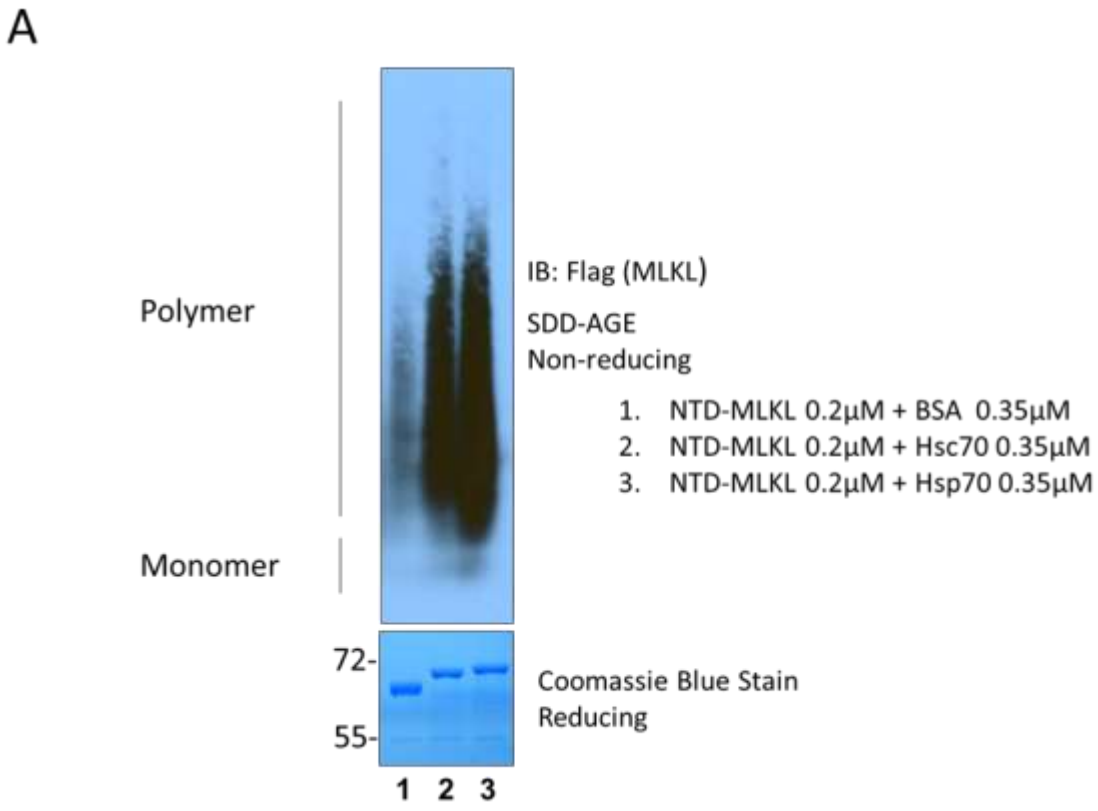

B

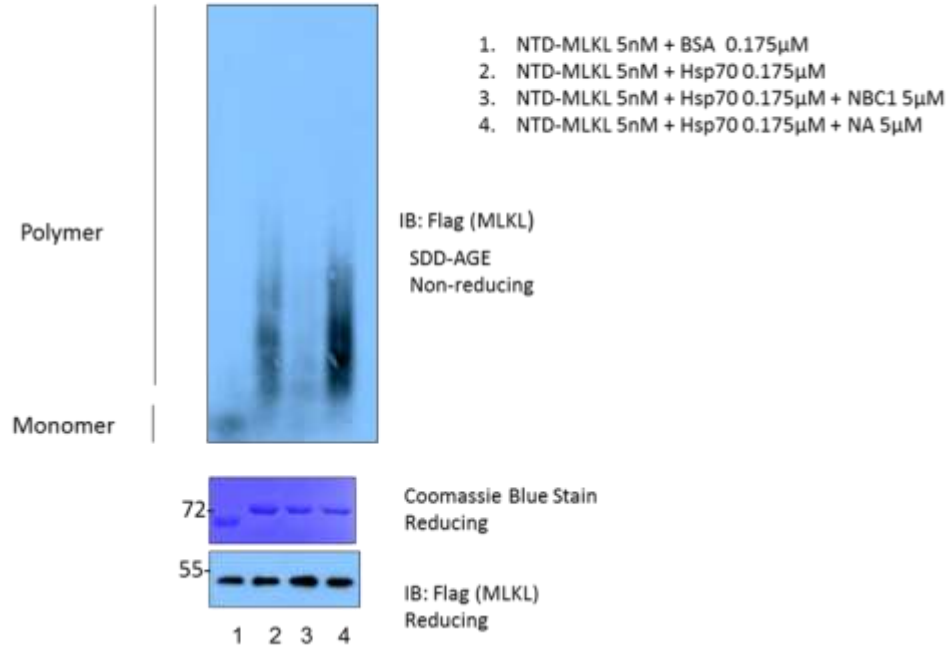
1. NTD-MLKL 5nM + BSA 0.175μM
2. NTD-MLKL 5nM + Hsp70 0.175μM
3. NTD-MLKL 5nM + Hsp70 0.175μM + NBC1 5μM
4. NTD-MLKL 5nM + Hsp70 0.175μM + NA 5μM
Polymer
Monomer
IB: Flag (MLKL)
SDD-AGE
Non-reducing
72
55
Coomassie Blue Stain
Reducing
IB: Flag (MLKL)
Reducing
1 2 3 4

C

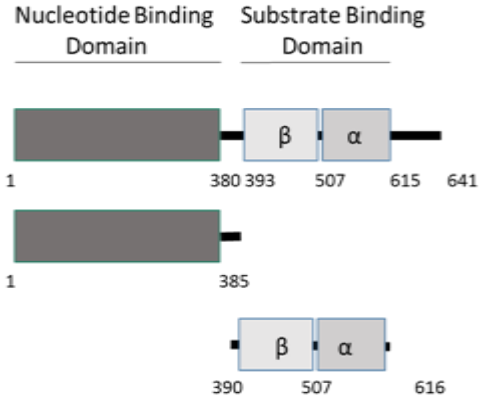
Nucleotide Binding Domain
Substrate Binding Domain
β
α
1
380
393
507
615
641
1
385
β
α
390
507
616

D

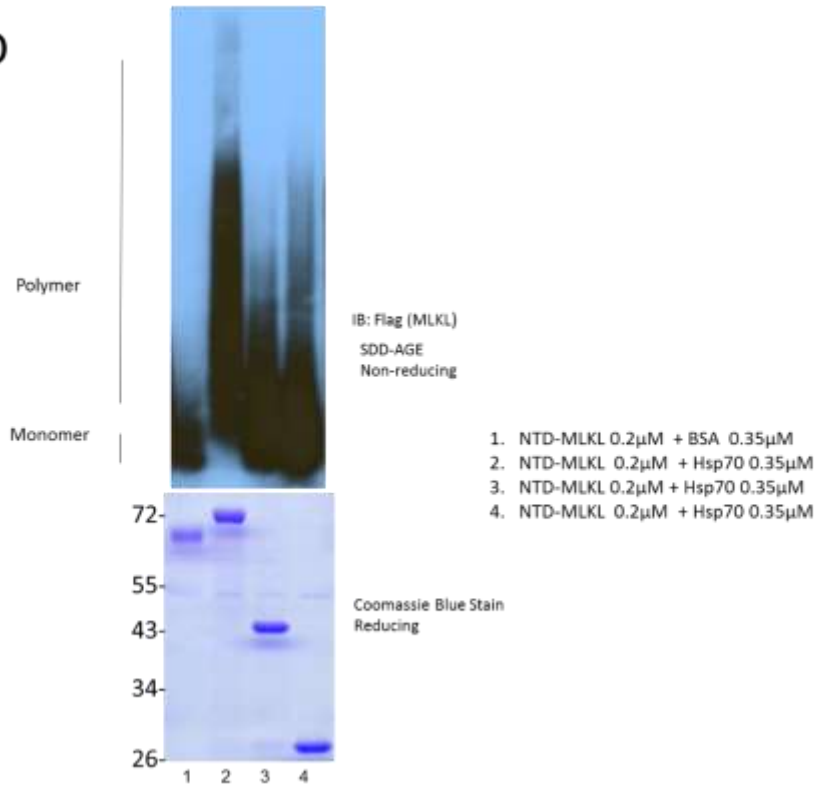
Polymer
Monomer
IB: Flag (MLKL)
SDD-AGE
Non-reducing
1. NTD-MLKL 0.2μM + BSA 0.35μM
2. NTD-MLKL 0.2μM + Hsp70 0.35μM
3. NTD-MLKL 0.2μM + Hsp70 0.35μM
4. NTD-MLKL 0.2μM + Hsp70 0.35μM
72-
55-
43-
34-
26-
1 2 3 4
Coomassie Blue Stain
Reducing

E

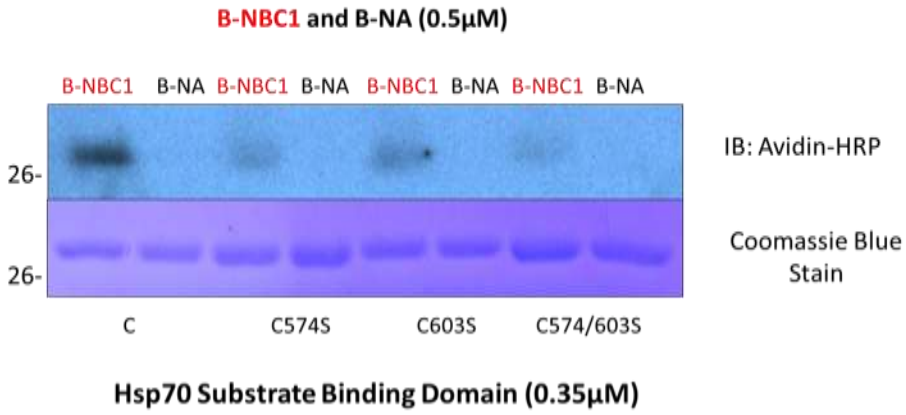
B-NBC1 and B-NA (0.5μM)
B-NBC1 B-NA B-NBC1 B-NA B-NBC1 B-NA B-NBC1 B-NA
26-
26-
IB: Avidin-HRP
Coomassie Blue Stain
C
C574S
C603S
C574/603S
Hsp70 Substrate Binding Domain (0.35μM)

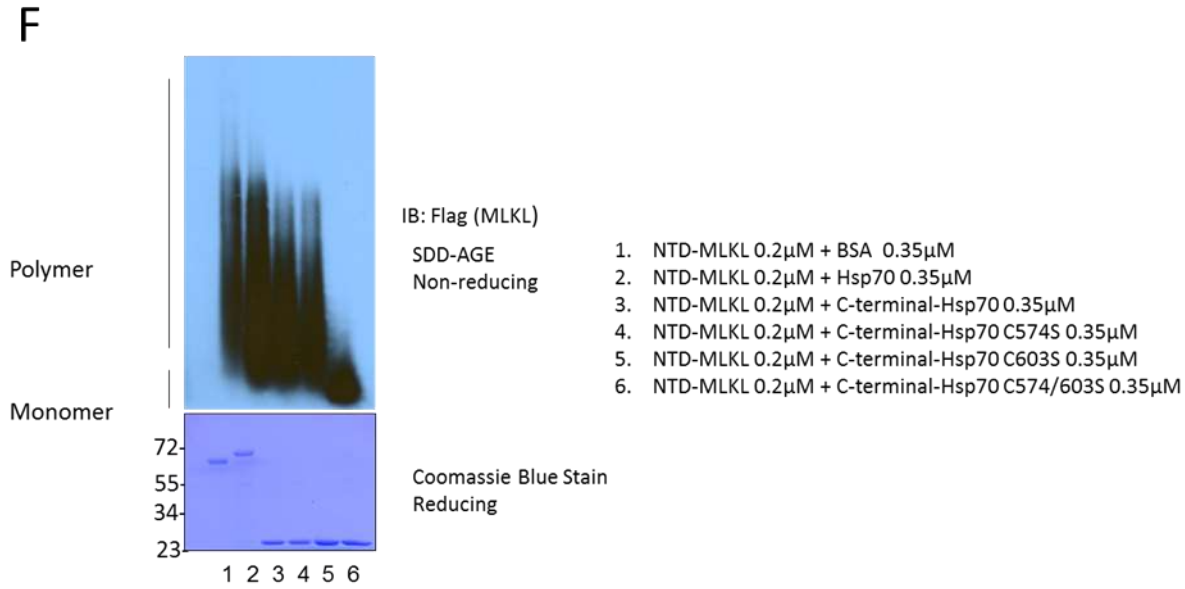

Figure 3.4. Hsp70 interacts directly with MLKL and enhances MLKL polymerization.
(A) Hsp70 enhances MLKL polymerization *in vitro*. Recombinant human N-terminus MLKL labeled with GST and Flag (NTD-MLK) combined with bovine serum albumin (BSA), recombinant human Hsp70 (Hsp70), or recombinant human Hsc70 as indicated were incubated at 23°C for 3 hours. The samples were separated by non-reducing SDD-AGE (upper panel) and protein loading was visualized by Coomassie blue staining (lower panel). NTD-MLK is just below 55kDa.
(B) NBC1 abrogates Hsp70 enhanced MLKL polymerization *in vitro*. NBC1 and NA were incubated with rhHsp70 for 24 hours at 4°C, then dialyzed in PBS for 16 hours at 4°C. BSA and Hsp70 were exposed to identical conditions. Samples were incubated with NTD-MLK as indicated at 23°C for 1 hour. The samples were separated by non-reducing SDD-AGE (upper panel) and protein loading was visualized by Coomassie blue staining (BSA, Hsp70) and Western blot (NTD-MLK) using anti-Flag antibody. NTD-MLKL 5nM is not visible with Coomassie blue staining.
(C) Domain structures of Hsp70 used for recombinant truncation proteins.
(D) Substrate binding domain of Hsp70 enhances MLKL polymerization *in vitro*. NTD-MLK combined with BSA, Hsp70, or recombinant human N-terminus nucleotide binding domain of Hsp70 (NTD) and C-terminus substrate binding domain of Hsp70 (SBD) at concentrations indicated were incubated at 23°C for 3 hours. The samples were separated by non-reducing SDD-AGE (upper panel) and protein loading was visualized by Coomassie blue staining (lower panel). NTD-MLK is just below 55kDa.
(E) Cysteine mutagenesis of the SBD decreases B-NBC1 affinity. *In vitro* conjugation assay was conducted with B-NBC1 or B-NA with the SBD and cysteine

to serine mutants of the SBD (C574S, C603S, C574/603S) at concentrations indicated, as described in experimental procedures. Samples were boiled in SDS loading buffer, separated on a polyacrylamide gel, and subjected to Western blot with avidin-HRP. Proteins were quantited by Coomassie blue stain.
(F) Cysteine mutagenesis of the SBD diminished MLKL polymerization *in vitro*. NTD-MLK was incubated with BSA, Hsp70, or cysteine to serine mutants of the SBD (C574S, C603S, C574/603S) at concentrations indicated at 23°C for 3 hours. The samples were separated by non-reducing SDD-AGE (upper panel) and protein loading was visualized by Coomassie blue staining (lower panel). NTD-MLK is just below 55kDa.

Hsp70 knockdown blocks necroptosis and destabilizes MLKL

Heat shock protein 70 is an inducible molecular chaperone responsible for protein folding and stability.[14,15] In order to evaluate whether reduction of Hsp70 inhibited necroptosis, Hsp70 was knocked down with small interfering RNA (siRNA). Concurrent treatment with the pan caspase inhibitor ZVAD-FMK was required to block apoptosis induced with Hsp70 knockdown. In NTD-DmrB cells and HeLa cells, stably transfected with RIPK3 and expressing endogenous MLKL, knockdown of Hsp70 effectively blocked necroptosis (Fig. 3.5A and Supplementary Fig. S2); however, Hsp70 knockdown modulates MLKL stability in cell lines with transgenic and endogenous MLKL expression (Fig. 3.5B and Supplementary Fig. S3). The MLKL protein was not found in the membrane fraction nor was a large protein aggregate identified in low percentage gel electrophoresis (data not shown). This finding is consistent with MLKL's client protein status but to confirm that the depletion was post-translational, Hsp70 and MLKL mRNA was measured following knockdown (Fig. 3.5C). MLKL mRNA was not reduced with Hsp70 knockdown but rather slightly increased suggesting translational or post-translational disruption of

MLKL. Notably, knockdown of Hsp70 did not affect RIPK1 or RIPK3 levels (Supplementary Fig. S3). Due to the high sequence homology between Hsp70 and the constitutively expressed Hsc70 and the importance of Hsp70's co-chaperone heat shock protein 40 (Hsp40, DNAJB1), the protective nature of these proteins were assessed by knockdown (Fig. 3.5D, E and Supplementary Fig. S4). Neither Hsc70 nor Hsp40 knockdown was protective against necroptotic cell death, suggesting that this effect is specific to Hsp70 and the potential that an alternate cochaperone, such as DNAJC7 or BAG5, is involved in protection. Unlike Hsp90, small molecule inhibition of Hsp70 with NBC1 at the duration and concentration required to protect from necroptosis did not diminish MLKL levels (Fig. 3.5F).[9,13] It is probable that MLKL instability is not integral to the necroptotic blocking function of NBC1 that limits MLKL polymerization.

A

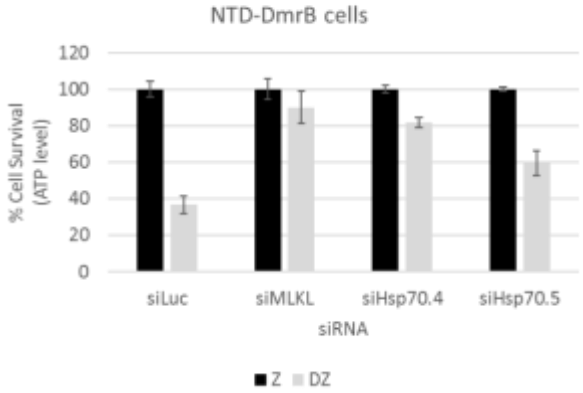
NTD-DmrB cells
% Cell Survival (ATP level)
120
100
80
60
40
20
0
siLuc
siMLKL
siHsp70.4
siHsp70.5
siRNA
Z
DZ

B

NTD-DmrB

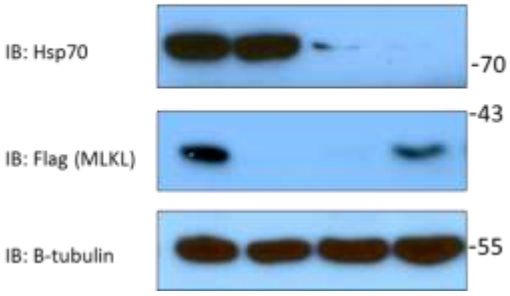
IB: Hsp70
-70
IB: Flag (MLKL)
-43
IB: B-tubulin
-55

C

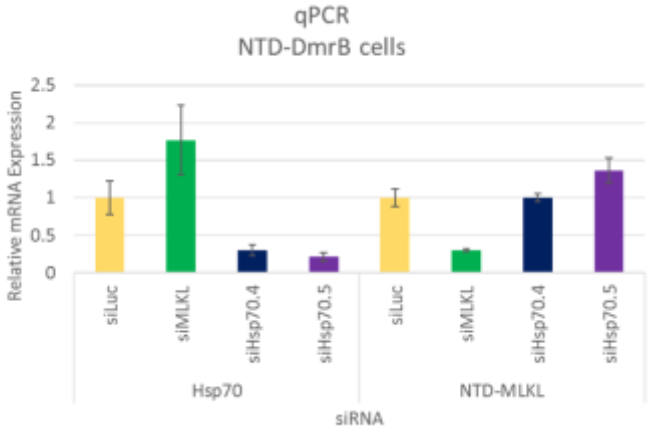
qPCR
NTD-DmrB cells
Relative mRNA Expression
2.5
2
1.5
1
0.5
0
siLuc
siMLKL
siHsp70.4
siHsp70.5
siLuc
siMLKL
siHsp70.4
siHsp70.5
Hsp70
NTD-MLKL
siRNA

D

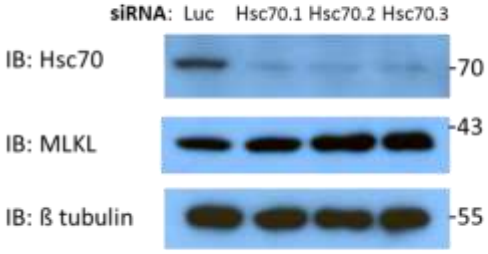
siRNA: Luc Hsc70.1 Hsc70.2 Hsc70.3
IB: Hsc70
-70
IB: MLKL
-43
IB: ß tubulin
-55

E

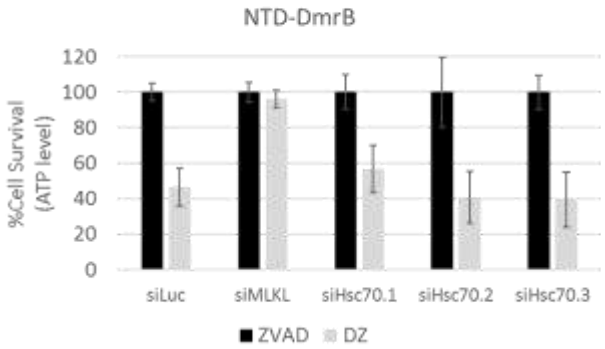
NTD-DmrB
%Cell Survival (ATP level)
120
100
80
60
40
20
0
siLuc
siMLKL
siHsc70.1
siHsc70.2
siHsc70.3
ZVAD
DZ

F

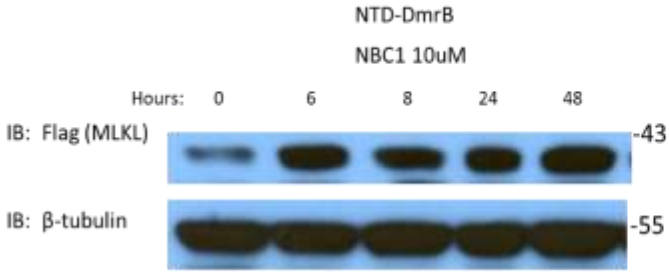
NTD-DmrB
NBC1 10uM
Hours: 0 6 8 24 48
IB: Flag (MLKL)
-43
IB: β-tubulin
-55

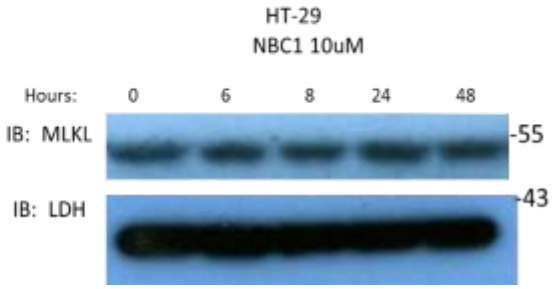
HT-29
NBC1 10uM
Hours: 0 6 8 24 48
IB: MLKL
-55
IB: LDH
-43

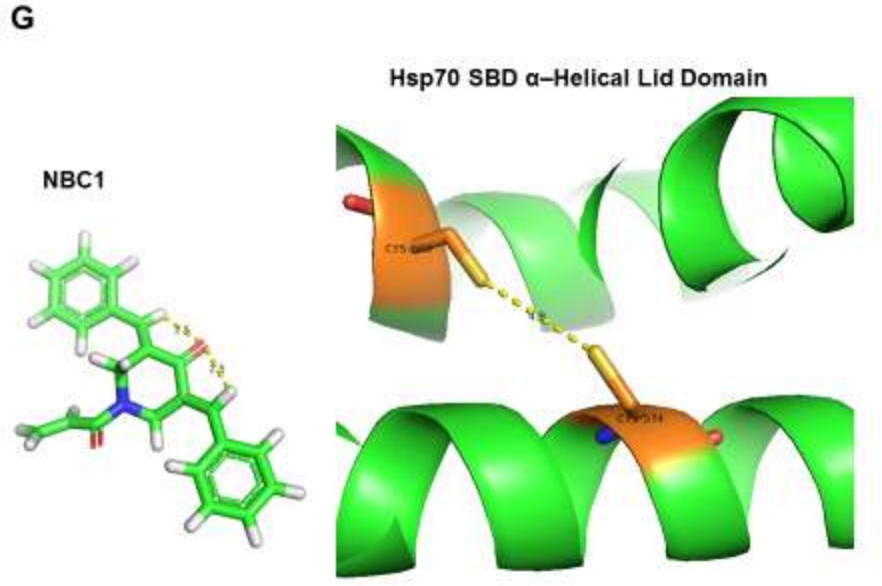

Figure 3.5. Hsp70 knockdown destabilizes MLKL.
(A) Knockdown of Hsp70 inhibits necroptosis. NTD-DmrB cells were transfected with siRNA against luciferase (siLuc), MLKL (siMLKL), or Hsp70 (siHsp70) with two different oligos (siHsp70.4 and 70.5) for 72 hours. Cells were treated with ZVAD-FMK (Z) and/or dimerizer (DZ) to induce necroptosis for 6 hours. Cell viability was measured with the CellTiter-Glo assay. Data are represented as mean ± SD of duplicates.
(B) Knockdown of Hsp70 destabilizes MLKL. NTD-DmrB cells were transfected with siRNA as indicated in 5A. Cell lysates were generated and knockdown of Hsp70 and MLKL was assessed by Western blot analysis with anti-Hsp70 and anti-Flag antibodies, respectively. Anti-β-tubulin immunoblot was used as a loading control. Data are representative of three replicates.
(C) Knockdown of Hsp70 does not diminish MLKL mRNA levels. NTD-DmrB cells were transfected with siRNA as indicated in 5A. RNA isolation, cDNA generation, and qPCR methods are described in experimental procedures. Sample relative mRNA expression is normalized to actin expression and Hsp70 and MLKL expression is normalized to cells transfected with si-luciferase (siLuc). Data is represented as mean ± SD of triplicate wells.
(D) Knockdown of Hsc70 does not inhibit necroptosis. NTD-DmrB cells were transfected with siRNA against luciferase (siLuc), MLKL (siMLKL), or Hsc70 (siHsp70) with three different oligos (siHsc70.1, 70.2, and 70.3) for 72 hours. Cells

were treated with ZVAD-FMK (Z) and/or dimerizer (DZ) to induce necroptosis for 6 hours. Cell viability was measured with the CellTiter-Glo assay. Data are represented as mean ± SD of triplicate wells.
(E) Knockdown of Hsc70 does not modulate MLKL stability. NTD-DmrB cells were transfected with siRNA as indicated in 5D. Cell lysates were generated and knockdown of Hsc70 and MLKL was assessed by Western blot analysis with anti-Hsc70 and anti-Flag antibodies, respectively. Anti-β-tubulin immunoblot was used as a loading control.
(F) NBC1 treatment does not reduce MLKL levels in NTD-DmrB or HT-29 cells. NTD-DmrB and HT-29 cells were treated with 10μM NBC1 for indicated intervals. Cell lysates were generated, separated on SDS-PAGE, and subjected to Western blot with MLKL and β-tubulin or LDH, as a loading controls. The low level of MLKL at 0 hours in NTD-DmrB cells likely reflect difference in dox protein induction.
(G) Mechanistic model of NBC1 conjugation of Hsp70. Cysteine residues 574 and 603 spanning 4.9 Ångstroms in the SBD of Hsp70. NBC1 molecule spans ~5.6 Ångstroms between Michael acceptors. A single molecule could covalently bind both cysteines. Hsp70 image generated with PyMOL from crystal structure 4PO2.

S1

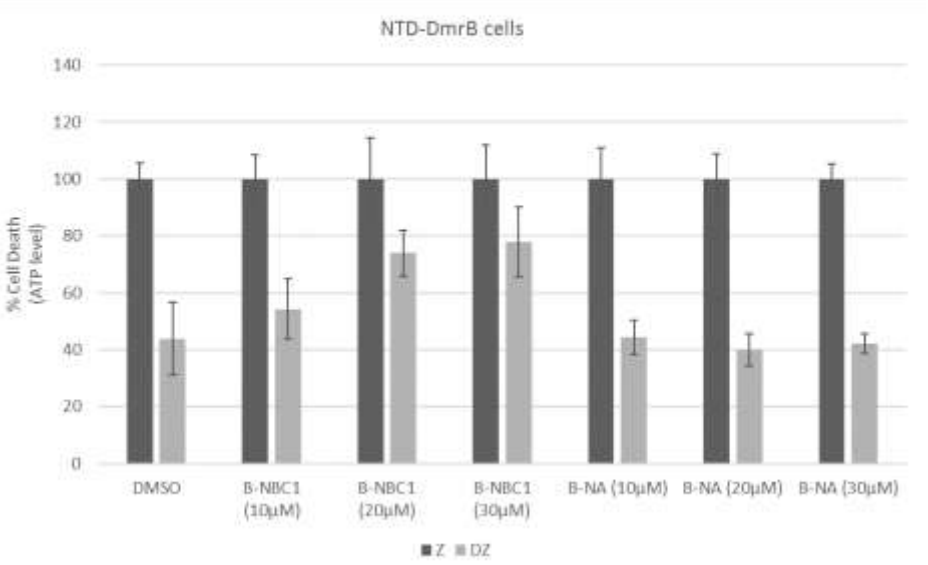

S2

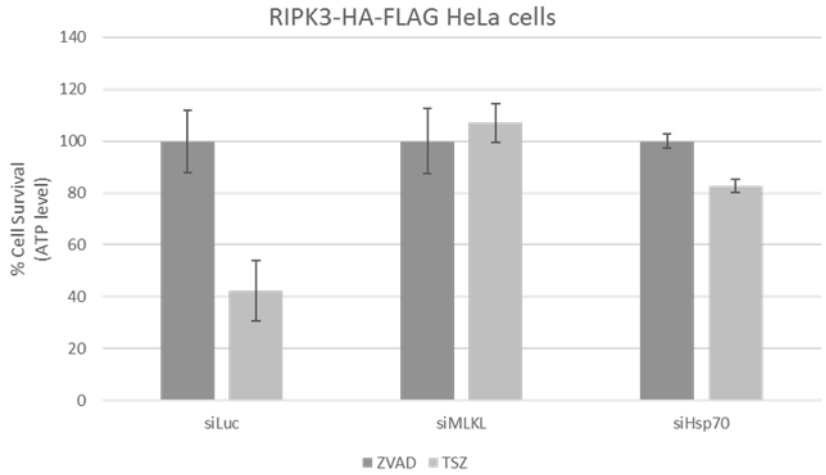
RIPK3-HA-FLAG HeLa cells
% Cell Survival (ATP level)
140
120
100
80
60
40
20
0
siLuc
siMLKL
siHsp70
ZVAD
TSZ

S3

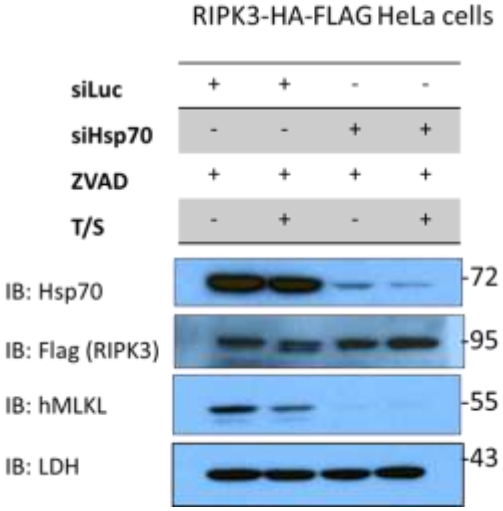
RIPK3-HA-FLAG HeLa cells
siLuc + + - -
siHsp70 - - + +
ZVAD + + + +
T/S - + - +
IB: Hsp70
IB: Flag (RIPK3)
IB: hMLKL
IB: LDH
72
95
55
43

S4

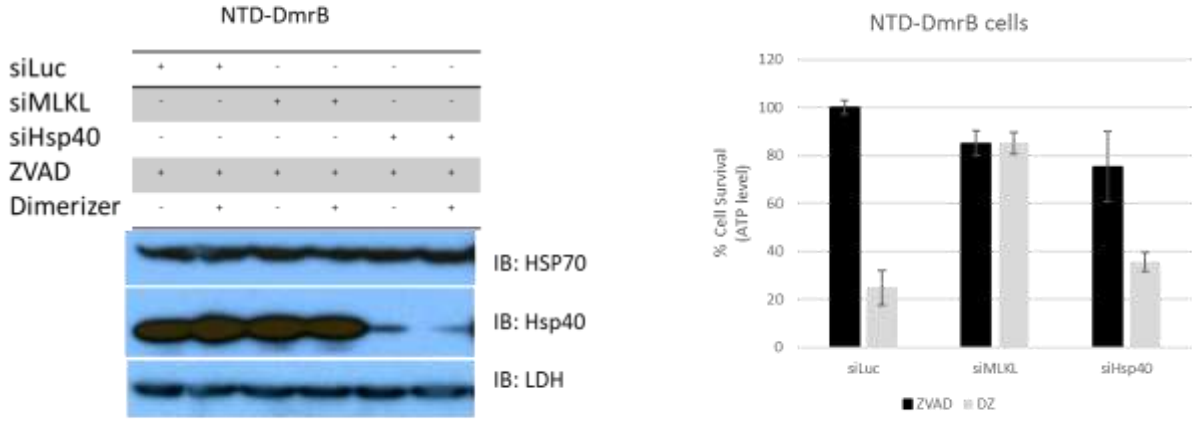

Supplemental Data

(S1) NTD-DmrB cells were treated with DMSO, B-NBC1, and B-NA. Necroptosis was induced by the addition of dimerizer and ZVAD-FMK (DZ). Cell survival was assessed by the CellTiter-Glo assay. Data are presented as mean ± SD.

(S2) Knockdown of Hsp70 inhibits necroptosis. HeLa GFP-RIPK3-FLAG cells that express endogenous MLKL were transfected with siRNA against luciferase (siLuc), MLKL (siMLKL), or Hsp70 (siHsp70.4) for 72 hours. Cells were treated with ZVAD-FMK (Z) and/or TNFα and Smac mimetic (TSZ) to induce necroptosis for 6 hours. Cell viability was measured with the CellTiter-Glo assay. Data are represented as mean ± SD of triplicate wells.

(S3) Knockdown of Hsp70 destabilizes endogenous MLKL HeLa GFP-RIPK3-FLAG cells were transfected with siRNA as indicated in Fig. S2. Cell lysates were generated and knockdown of Hsp70 and MLKL was assessed by Western blot analysis with anti-Hsp70 and anti-Flag antibodies, respectively. RIPK3, Phospho-MLKL, and LDH expression were also evaluated by immunoblot.

(S4) Knockdown of Hsp40 (DNAJB1) does not inhibit necroptosis. Left panel: NTD-DmrB cells were transfected with siRNA against luciferase (siLuc), MLKL (siMLKL), or Hsp40 (siHsp40) for 72 hours. Cell lysates were generated and knockdown of Hsp40 was assessed by Western blot analysis with anti-Hsp40 antibody. Anti-LDH immunoblot was used as a loading control. Anti-Hsp70 antibody immunoblot was performed to ensure stability. Right panel: Cells were treated with ZVAD-FMK (Z) and/or dimerizer (DZ) to induce necroptosis for 6 hours. Cell viability was measured with the CellTiter-Glo assay. Data are represented as mean ± SD of triplicate wells.

Discussion

The results herein identify a novel small molecule inhibitor of necroptosis, NBC1, effective in human colon adenocarcinoma (HT-29), human cervical carcinoma (HeLa), and murine fibrosarcoma (L929) cell lines. NBC1 targets the stress inducible molecular chaperone Hsp70. Through this interaction, Hsp70 has been identified as a novel-MLKL interacting protein. Mechanisticaly, chemical inhibition of Hsp70 necroptotic cell death by abrogating MLKL polymerization, a necessary step in necroptosis. *In vitro,* Hsp70 enhances MLKL polymerization and this effect is inhibited when Hsp70 is pretreated with NBC1.

Hsp70 regulates many eukaryotic proteins through transient association.[16] These include nuclear receptors (steroid hormone receptors), kinases (Raf, eIF2α-kinase) and transcription factors (HSF, c-Myc, pRb). In these complexes, chaperone binding is sensitive to substrate-ligands or substrate phosphorylation. Some proteins, often eukaryotic kinases, use the Hsp70 and Hsp90-co-chaperone (Cdc37) system pathways in tandem.[16-18] Hsp70's function in necroptosis is similar to that previously reported for Hsp90, in that both molecular chaperones interact with MLKL and modulate the formation of high molecular weight MLKL oligomers.[4,19] Unlike Hsp90, Hsp70 mediates its pro-necroptotic effect through the N-terminus domain of MLKL. Hsp90 interacts with both the N and C terminuss, Hsp90 inhibition was unable to block necroptosis induced by the N-terminus 4HB alone.[4,6] Further, Hsp90 facilitates tetramer formation, which is unhindered with NBC1's inhibition of Hsp70. Hsp70 blocks MLKL polymerization after tetramer formation. This points to distinct

mechanisms of Hsp70 and 90 in regards to MLKL multimer stability. It is tempting to hypothesize that these molecular chaperones work together to ensure MLKL oligomer structural stability.

Knockdown of Hsp70 destabilized MLKL protein but did not disrupt mRNA levels, consistent with MLKL's client protein status. Yet, small molecule inhibition of Hsp70 with NBC1 did not modulate MLKL protein levels in HeLa or HT-29 cells. This may be due to the more profound effects of Hsp70 knockdown on protein translation or post-translational modifications than chemical inhibition alone. Alternatively, Hsp70 may stabilize an intermediary molecular chaperone of MLKL. Chemical inhibition of Hsp90 does not consistently reduce levels of its client proteins RIPK1, RIPK3, or MLKL and this is reportedly dependent on specific inhibitors and the cell lines utilized.[4,5,7,20] The percent of cell survival and effective concentration of NBC1 varied between cell lines. Mouse L929 cells had a fifteen-fold higher EC_{50} than HT-29 cells, illustrating potential species and tissue differences that may be relevant to Hsp70 signal regulation in necroptosis.

Hsp70 and its constitutively expressed family member heat shock cognate 70 (Hsc70) share a high degree of structural and sequence homology. The *in vitro* polymerization of MLKL by both Hsp70 and Hsc70 suggests that they are functionally equivalent, but Hsc70 knockdown did not prevent necroptosis nor modulate MLKL levels when used in cellular necroptosis cell death assays. Mechanistic differences between Hsc70 and Hsp70 clearly exist *in vivo* and may be attributed to interactions with other protein mediators or distinct co-chaperones.

Interestingly, the knockdown of the Hsp70 cofactor Hsp40 (DNAJB1), which stimulates Hsp70's ATPase activity, had no effect on necroptosis. An alternative co-chaperone is likely involved but remains to be identified.

NBC1 binds the C-terminal, SBD of Hsp70 and that interaction is disrupted when cysteine residues 574 and 603 are mutated to serine residues. The SBD is divided into two subdomains, a two-layer β-sandwich, containing the binding pocket, and α helical lid subdomain, composed of five helices (A-E) and terminating in an intrinsically disordered region. Both cysteine residues are located in the α-helical lid domain (residues 508-641), which regulates the kinetics of substrate binding and can induce conformational changes in bound substrate.[21] Cysteine mutagenesis of Hsp70 SBD limits MLKL polymerization *in vitro*. While the lid is required for Hsp70 function, ATPase activity is not universally required.[21-24] Previous studies indicate that the truncated Hsp70 SBD is able to bind substrates independently of the NTD in the nucleotide free state. The lid does not need to fold over the substrate, allowing multiple sizes of substrate to bind.[25] I hypothesize that small molecule blockade of the cysteine residues in the α helical lid subdomain of Hsp70 modulate lid mobility and reducing affinity for the MLKL and, or eliminating Hsp70's ability to enhance MLKL polymerization (Fig. 3.5G). When bound to substrate, cysteine 574 and 603 are approximately 4.9 Ångstroms apart. These cysteines reside in helices C and D. It is uncertain if these regions would have direct contact with substrate when within Hsp70 the binding pocket, but the covalent linkage o NBC1 may potentially limit α helical lid mobility or modulate binding affinity, particularly in a multimeric molecule.

Structural data of the MLKL polymer bound or unbound to NBC1 would be helpful to validate this hypothesis. Additional *in vivo* necroptosis survival analysis of cysteine mutagenized Hsp70 would also be worthwhile. This may be technically challenging in neoplastic cell lines as knockdown of Hsp70 results in apoptosis when caspases are not inihibited and MLKL is destabilized. Alternative strategies using base editing have been considered but cysteine 574 lacks an appropriate PAM site to direct currently available base editors. Knockout and stable transfection of a mutagenized Hsp70 may be more feasible in non-transformed cell lines or primary murine culture, as $Hsp70^{-/-}$ mice are viable.

References

1. Degterev, A.*, et al.* Chemical inhibitor of nonapoptotic cell death with therapeutic potential for ischemic brain injury. *Nat Chem Biol* **1**, 112-119 (2005).
2. Sun, L.*, et al.* Mixed lineage kinase domain-like protein mediates necrosis signaling downstream of RIP3 kinase. *Cell* **148**, 213-227 (2012).
3. Zhao, X.M.*, et al.* Hsp90 modulates the stability of MLKL and is required for TNF-induced necroptosis. *Cell Death Dis* **7**, e2089 (2016).
4. Jacobsen, A.V.*, et al.* HSP90 activity is required for MLKL oligomerisation and membrane translocation and the induction of necroptotic cell death. *Cell Death Dis* **7**, e2051 (2016).
5. Li, D.*, et al.* Natural Product Kongensin A is a Non-Canonical HSP90 Inhibitor that Blocks RIP3-dependent Necroptosis. *Cell Chem Biol* **23**, 257-266 (2016).
6. Jacobsen, A.V. & Silke, J. The importance of being chaperoned: HSP90 and necroptosis. *Cell Chem Biol* **23**, 205-207 (2016).
7. Li, D.*, et al.* A cytosolic heat shock protein 90 and cochaperone CDC37 complex is required for RIP3 activation during necroptosis. *Proc Natl Acad Sci U S A* **112**, 5017-5022 (2015).
8. Wang, Z., Jiang, H., Chen, S., Du, F. & Wang, X. The mitochondrial phosphatase PGAM5 functions at the convergence point of multiple necrotic death pathways. *Cell* **148**, 228-243 (2012).
9. Reynoso, E.*, et al.* Thioredoxin-1 actively maintains the pseudokinase MLKL in a reduced state to suppress disulfide bond-dependent MLKL polymer formation and necroptosis. *J Biol Chem* (2017).

10. Budina-Kolomets, A.*, et al.* Comparison of the activity of three different HSP70 inhibitors on apoptosis, cell cycle arrest, autophagy inhibition, and HSP90 inhibition. *Cancer Biol Ther* **15**, 194-199 (2014).
11. Balaburski, G.M.*, et al.* A modified HSP70 inhibitor shows broad activity as an anticancer agent. *Mol Cancer Res* **11**, 219-229 (2013).
12. Halfmann, R. & Lindquist, S. Screening for amyloid aggregation by Semi-Denaturing Detergent-Agarose Gel Electrophoresis. *J Vis Exp* (2008).
13. Liu, S.*, et al.* MLKL forms disulfide bond-dependent amyloid-like polymers to induce necroptosis. *Proc Natl Acad Sci U S A* (2017).
14. Sekhar, A., Rosenzweig, R., Bouvignies, G. & Kay, L.E. Hsp70 biases the folding pathways of client proteins. *Proc Natl Acad Sci U S A* **113**, E2794-2801 (2016).
15. Cesa, L.C.*, et al.* X-linked inhibitor of apoptosis protein (XIAP) is a client of heat shock protein 70 (Hsp70) and a biomarker of its inhibition. *J Biol Chem* **293**, 2370-2380 (2018).
16. Mayer, M.P. & Bukau, B. Hsp70 chaperones: cellular functions and molecular mechanism. *Cell Mol Life Sci* **62**, 670-684 (2005).
17. Jaattela, M. Heat shock proteins as cellular lifeguards. *Ann Med* **31**, 261-271 (1999).
18. Hartl, F.U. & Hayer-Hartl, M. Molecular chaperones in the cytosol: from nascent chain to folded protein. *Science* **295**, 1852-1858 (2002).
19. Yang, C.K. & He, S.D. Heat shock protein 90 regulates necroptosis by modulating multiple signaling effectors. *Cell Death Dis* **7**, e2126 (2016).
20. Chen, W.W.*, et al.* RIP1 mediates the protection of geldanamycin on neuronal injury induced by oxygen-glucose deprivation combined with zVAD in primary cortical neurons. *J Neurochem* **120**, 70-77 (2012).
21. Mayer, M.P.*, et al.* Multistep mechanism of substrate binding determines chaperone activity of Hsp70. *Nat Struct Biol* **7**, 586-593 (2000).
22. Arlet, J.B.*, et al.* HSP70 sequestration by free alpha-globin promotes ineffective erythropoiesis in beta-thalassaemia. *Nature* **514**, 242-246 (2014).
23. Ribeil, J.A.*, et al.* Hsp70 regulates erythropoiesis by preventing caspase-3-mediated cleavage of GATA-1. *Nature* **445**, 102-105 (2007).
24. Boudesco, C., Cause, S., Jego, G. & Garrido, C. Hsp70: A Cancer Target Inside and Outside the Cell. *Methods Mol Biol* **1709**, 371-396 (2018).
25. Schlecht, R., Erbse, A.H., Bukau, B. & Mayer, M.P. Mechanics of Hsp70 chaperones enables differential interaction with client proteins. *Nat Struct Mol Biol* **18**, 345-351 (2011).

CHAPTER FOUR
Discussion

Relevance of necroptosis

Necroptosis is a caspase-independent, immunogenic subtype of regulated cell death. Necroptosis is a fail-safe cell death subroutine that proceeds as an alternative to apoptosis when caspase activation is inhibited. Some researchers have hypothesized that this pathway has co-evolved as a pathogen defense mechanism.[1-4] Many viridae are capable of bypassing apoptosis to avoid host clearance.[5] Virally evolved mechanisms of defense are variable. Murine and human cytomegalovirus (CMV) encode vICA (viral inhibitor of caspase 8) blocking apoptosis to persist in macrophages and monocytes. Herpes virus and poxvirus encode vFLIP-like proteins, which share homology with cellular death effector domains such as FADD and procaspase 8. These too inhibit apoptosis either by preventing FADD oligomerization or caspase 8 activation.[6,7] These inhibitory pathways stimulate RIPK1 driven necroptosis, limiting viral replication and stimulating innate, and ultimately adaptive, immune responses.

Despite the pro-inflammatory effects of necroptotic death this response is beneficial to the organism as a whole. Illustrating this point, RIPK3$^{-/-}$ mice and RIPK1-D138N kinase dead knock-in mice have less tissue damage with vaccinia infection but have higher viral titers. The unchecked viral replication leads to death although the virus does not kill wild-type mice.[8]

Pathogens have also evolved mechanisms to hinder necroptosis. Murine cytomegalovirus M45 protein blocks necroptosis by disturbing the RIPK1 RHIM domain. When the CMV M45 RHIM interacting domain is mutagenized, CMV fails to replicate; however, CMV evades this replication failure when host RIPK3 is knocked-out, suggesting that RIPK3 dependent necroptosis prevents replication.[9-11] Herpes simplex virus 1 (HSV-1) is an example with species dichotomy. HSV-1 encodes ICP6 RHIM interacting protein, which blocks RIPK1/3 interaction and necroptotic cell death in human cells. Contrarily in murine cells the same protein triggers necrosome formation, promoting necroptosis.[12,13] The theory of pathogen-host cell death adaptive evolution has been challenged as the core components of necroptosis, RIPK3 and MLKL, are not well conserved among Metazoans.[14]

RIPK3 and MLKL are present in reptiles, but birds lack RIPK3. Among mammals, RIPK3 and MLKL are absent in marsupials and order Carnivora, including *Canis familiaris* and *Felis catus*, lacks MLKL. This is unusual because domestic dogs and cats share many human pathogens and pathogeneses. These distinct evolutionary patterns may be driven by the detrimental effects of necroptosis in embryogenesis.[13] There is an important molecular interplay between the regulated cell death pathways during development, which seems to depend on caspase-8 level and activity. Deletion of negative regulators of necroptosis in mice (FADD or caspase 8) leads to embryonic lethality at least in part caused by necroptosis.[15-17] Exposure *in utero* to high pathogen levels from the carnivore diet may impart a survival benefit to species unable to undergo necroptosis.[14] Alternatively, a parallel

cell death pathway may exist in these species. I hope to direct future research efforts towards defining TNF mediated cell death in carnivores. The biochemical techniques learned in my graduate studies will be directly applicable.

Hsp70 and the MLKL polymer

My graduate work has resulted in identification of the polymeric form of full length MLKL and recombinant NTD MLKL by electron microscopy. This result validated the biochemical data that MLKL forms a structural polymer following induction of necroptosis and confirmed that the polymer can form from the MLKL 4HB and brace domain *in vitro* when the inhibitory pseudokinase domain is absent. Further, I have also identified a novel small molecule inhibitor of necroptosis (NBC1), which conjugates Hsp70. Hsp70 inhibits necroptosis through its interaction with MLKL. Hsp70 promotes MLKL oligomerization *in vitro* and in cell culture and NBC1 inhibits that effect.

The primary role of chaperone proteins is to interact with nascent polypeptides to accelerate folding, but they are also involved in protein translocation, translation, and rescue of misfolded and aggregated proteins that occur secondary to cell stress. In some instances, chaperones remodel mammalian and fungal proteins into multiprotein complexes or organized, protease resistant fibers or prions, preventing protein aggregation.[18-20] Despite its ambiguous role in prion propagation, Hsp70 has been labelled the quintessential inhibitor of cell death due to its maintenance of native and biologically active protein forms.[21-28] This perspective

calls into question why a molecular chaperone would promote necroptosis. It is possible that use of transformed cell lines, which grossly overexpress Hsp70 and have profoundly modulated cell death programs, have skewed these results.

Previous publications have shown a divergent function for Hsp70 in necroptosis. [29,30] Chemical inhibition of Hsp70's NBD with the allosteric inhibitor JG-98 and analogs destabilizes RIPK1 regulators (cIAP1/2, XIAP, and $cFLIP_{S/L}$), causing apoptosis and, with caspase inhibition, necroptosis. These studies were conducted in breast cancer cell lines (MDA-MB-231, MCF7, SK-BR-3) and Jurkat cells; however, variable results were reported in A549 (lung), T47-D (breast), and HT-29 (colon) cells wherein co-treatment with JG-98, ZVAD-FMK, and the MLKL inhibitor, NSA did not block cell death. This suggests that an alternate RCD pathway may be involved in JG-98 mediated cell death in some cell types. Hsp70 has also found to promote cytotoxicity when complexed with Tag7, a known inhibitor of TNF activation through TNFR1 binding. The Tag7-Hsp70 complex causes cell death in tumor cells via permeabilization of lysosomes and mitochondria.[31,32] Tag7-Hsp70 complex in L929 cells induced modest cell death that could be blocked by necrostatin-1, chloroquine, ionol (antioxidant), or excess Tag7.[33] Although this was suggested to be necroptotic cell death, the lysosome and mitochondrial dependence do not comply with the currently accepted necroptotic pathway, nor has involvement of RIPK3 or MLKL been documented.[31]

Many questions remain regarding the role of the stress response in cell death and specifically molecular chaperone function stabilizing and destablilizing amyloid-

like polymers. I hypothesize that Hsp70's regulation of MLKL polymerization reflects the basic proteostatic function of chaperone proteins. The *in vitro* data demonstrate that Hsp70 promotes MLKL polymerization and this can be inhibited by NBC1. MLKL polymerization may be a protective mechanism against membrane lysis from the MLKL monomer or tetrameric forms of MLKL. Determining the exact stoichiometry of the membrane disruptive MLKL protomers using imaging techniques such as cryo-electron microscopy will be key in determining exactly how cells die from necroptosis.

References

1. Brault, M. & Oberst, A. Controlled detonation: evolution of necroptosis in pathogen defense. *Immunol Cell Biol* **95**, 131-136 (2017).
2. Jorgensen, I., Rayamajhi, M. & Miao, E.A. Programmed cell death as a defence against infection. *Nat Rev Immunol* **17**, 151-164 (2017).
3. Pearson, J.S. & Murphy, J.M. Down the rabbit hole: Is necroptosis truly an innate response to infection? *Cell Microbiol* **19**(2017).
4. Saleh, D. & Degterev, A. Emerging Roles for RIPK1 and RIPK3 in Pathogen-Induced Cell Death and Host Immunity. *Curr Top Microbiol Immunol* **403**, 37-75 (2017).
5. Kaiser, W.J., Upton, J.W. & Mocarski, E.S. Viral modulation of programmed necrosis. *Curr Opin Virol* **3**, 296-306 (2013).
6. Shisler, J.L. Viral and cellular FLICE-inhibitory proteins: a comparison of their roles in regulating intrinsic immune responses. *J Virol* **88**, 6539-6541 (2014).
7. Glykofrydes, D.*, et al.* Herpesvirus saimiri vFLIP provides an antiapoptotic function but is not essential for viral replication, transformation, or pathogenicity. *J Virol* **74**, 11919-11927 (2000).
8. Veyer, D.L., Carrara, G., Maluquer de Motes, C. & Smith, G.L. Vaccinia virus evasion of regulated cell death. *Immunol Lett* **186**, 68-80 (2017).
9. Upton, J.W., Kaiser, W.J. & Mocarski, E.S. Cytomegalovirus M45 cell death suppression requires receptor-interacting protein (RIP) homotypic interaction motif (RHIM)-dependent interaction with RIP1. *J Biol Chem* **283**, 16966-16970 (2008).

10. Upton, J.W., Kaiser, W.J. & Mocarski, E.S. DAI/ZBP1/DLM-1 complexes with RIP3 to mediate virus-induced programmed necrosis that is targeted by murine cytomegalovirus vIRA. *Cell Host Microbe* **11**, 290-297 (2012).
11. Upton, J.W., Kaiser, W.J. & Mocarski, E.S. Virus inhibition of RIP3-dependent necrosis. *Cell Host Microbe* **7**, 302-313 (2010).
12. Huang, Z.*, et al.* RIP1/RIP3 binding to HSV-1 ICP6 initiates necroptosis to restrict virus propagation in mice. *Cell Host Microbe* **17**, 229-242 (2015).
13. Upton, J.W., Shubina, M. & Balachandran, S. RIPK3-driven cell death during virus infections. *Immunol Rev* **277**, 90-101 (2017).
14. Dondelinger, Y., Hulpiau, P., Saeys, Y., Bertrand, M.J.M. & Vandenabeele, P. An evolutionary perspective on the necroptotic pathway. *Trends Cell Biol* **26**, 721-732 (2016).
15. Shan, B., Pan, H., Najafov, A. & Yuan, J. Necroptosis in development and diseases. *Genes Dev* **32**, 327-340 (2018).
16. Feltham, R., Vince, J.E. & Lawlor, K.E. Caspase-8: not so silently deadly. *Clin Transl Immunology* **6**, e124 (2017).
17. Weinlich, R., Oberst, A., Beere, H.M. & Green, D.R. Necroptosis in development, inflammation and disease. *Nat Rev Mol Cell Biol* **18**, 127-136 (2017).
18. Jones, G.W. & Tuite, M.F. Chaperoning prions: the cellular machinery for propagating an infectious protein? *Bioessays* **27**, 823-832 (2005).
19. Schlecht, R., Erbse, A.H., Bukau, B. & Mayer, M.P. Mechanics of Hsp70 chaperones enables differential interaction with client proteins. *Nat Struct Mol Biol* **18**, 345-351 (2011).
20. Rohde, M.*, et al.* Members of the heat-shock protein 70 family promote cancer cell growth by distinct mechanisms. *Genes Dev* **19**, 570-582 (2005).
21. Safferthal, C., Rohde, K. & Fulda, S. Therapeutic targeting of necroptosis by Smac mimetic bypasses apoptosis resistance in acute myeloid leukemia cells. *Oncogene* **36**, 1487-1502 (2017).
22. Simon, M.M.*, et al.* Heat shock protein 70 overexpression affects the response to ultraviolet light in murine fibroblasts. Evidence for increased cell viability and suppression of cytokine release. *J Clin Invest* **95**, 926-933 (1995).
23. Ravagnan, L.*, et al.* Heat-shock protein 70 antagonizes apoptosis-inducing factor. *Nat Cell Biol* **3**, 839-843 (2001).
24. Nylandsted, J. & Jaattela, M. [Heat shock protein 70: an important survival factor for cancer cells]. *Ugeskr Laeger* **166**, 3184-3186 (2004).
25. Kirkegaard, T.*, et al.* Hsp70 stabilizes lysosomes and reverts Niemann-Pick disease-associated lysosomal pathology. *Nature* **463**, 549-553 (2010).
26. Jaattela, M., Wissing, D., Bauer, P.A. & Li, G.C. Major heat shock protein hsp70 protects tumor cells from tumor necrosis factor cytotoxicity. *EMBO J* **11**, 3507-3512 (1992).

27. Jaattela, M. & Wissing, D. Heat-shock proteins protect cells from monocyte cytotoxicity: possible mechanism of self-protection. *J Exp Med* **177**, 231-236 (1993).
28. Boudesco, C., Cause, S., Jego, G. & Garrido, C. Hsp70: A Cancer Target Inside and Outside the Cell. *Methods Mol Biol* **1709**, 371-396 (2018).
29. Srinivasan, S.R.*, et al.* Heat Shock Protein 70 (Hsp70) Suppresses RIP1-Dependent Apoptotic and Necroptotic Cascades. *Mol Cancer Res* **16**, 58-68 (2018).
30. Cesa, L.C.*, et al.* X-linked inhibitor of apoptosis protein (XIAP) is a client of heat shock protein 70 (Hsp70) and a biomarker of its inhibition. *J Biol Chem* **293**, 2370-2380 (2018).
31. Yashin, D.V., Romanova, E.A., Ivanova, O.K. & Sashchenko, L.P. The Tag7-Hsp70 cytotoxic complex induces tumor cell necroptosis via permeabilisation of lysosomes and mitochondria. *Biochimie* **123**, 32-36 (2016).
32. Yashin, D.V.*, et al.* Tag7 (PGLYRP1) in Complex with Hsp70 Induces Alternative Cytotoxic Processes in Tumor Cells via TNFR1 Receptor. *J Biol Chem* **290**, 21724-21731 (2015).
33. Degterev, A.*, et al.* Chemical inhibitor of nonapoptotic cell death with therapeutic potential for ischemic brain injury. *Nat Chem Biol* **1**, 112-119 (2005).

MATERIALS AND METHODS

General Reagents

Necroptosis blocking compound 1 (NBC1, NSC632841) was obtained from the National Cancer Institute (NCI)/Division of Cancer Treatment and Diagnosis (DCTD)/Developmental Therapeutics Program (DTP; http://dtp.cancer.gov). The Chuo Chen lab performed generation of compound analogues and Biotinylated compounds. Recombinant human TNFα, and Smac-mimetic were prepared as previously described (He, 2009). The following reagents and antibodies were used: ZVAD-FMK (ApexBio), recombinant mouse TNF (BioLegend), Necrosulfonamide (Millipore), Dimerizer (Clonetech, 635058), Anti-Flag M2 antibody and affinity gel (Sigma), Anti-human MLKL (Genetex, GTX107538), Anti-mouse MLKL (Aviva Systems Biology, OAAB10571), anti-phospho-MLKL S358 (Abcam, ab187091), anti-RIPK1 (BD, 551042), anti-LDH (Abcam, ab53292), anti-Hsp40 (Cell Signaling Technologies, 4868), and anti-Hsc70 (Santa Cruz, 1059, K-19), and monoavidin agarose (Pierce, 20228). Human cell lines were treated with recombinant human TNF (20ng/mL), Smac-mimetic (100nm), and ZVAD-FMK (20uM). Mouse endothelial fibroblasts were treated with recombinant human TNF (2ng/mL), Smac-mimetic (100nm), and ZVAD-FMK (20uM) and L929 cells were treated with TNF (2ng/mL). HeLa cells stably transfected with dimerizable MLKL 1-190 were treated with 20nM dimerizer and 20uM ZVAD-FMK. Cell death was standardly evaluated at 20 hours. For

compound treatment, NBC1 and the negative analog (NA, +/- biotynilation) were used at 10uM, PES-Cl was used at 5uM, NA, and necrosulfonamide (NSA) was used at 5uM.

Cell culture and cell lines

HT-29, HeLa, L929, and MEFs were cultured in DMEM (high glucose) supplemented with 10% FBS. All of the stable HeLa cell lines were generated in the background of the previously reported HeLa-TetR cells that expressed the Tet repressor (TetR).[1] For the MLKL-knockout, Tet-inducible GFP-RIPK3, Tet-inducible MLKL-C-HA-3xFlag, and NTD-DmrB HeLa lines were generated as previously described.[2] For all doxycycline (Dox) inducible stable lines, 50ng/mL Dox was added 24 hours prior to necroptosis induction to induce transgene expression. Cell lysates were used for Western blotting, SDD-AGE, or immunoprecipitation.

Small interfering RNA (siRNA) transfection

For siRNA transfection, cells were plated at 2,000 cells per well in 96-well plates and 100,000 cells per well in 6-well plates 24 hours prior to transfection. Transfection was carried out as per GenMute (SignaGen) protocol. Briefly, 1x GenMute Buffer was combined with 5nM (96 well)or 50nM (6 well) siRNA and incubated with GenMute reagent for 15 minutes at room temperature. Working solution was added dropwise to wells. Cells were incubated in standard culture

conditions for 24 to 48 hours prior to treatment. RNA oligos were generated by Sigma (siHsp40 (ACCCGUCGUAUUCAAAGAUGU), siHSC70 (CCGAACCACUCCAAGCUAU), siHsp70.4 (UGACCAAGAUGAAGGAGAU), siHsp70.5(AGAAGAAGGTGCTGGACAA), siMLKL1-190.1 (GCUAAGAAGAGAUAAUGAA) and siMLKL190.2 (GCUAAUGGGGAGAUAGAA). Knockdown was measured by Western blot.

Non-reducing SDS/PAGE

Non-reducing SDS/PAGE is as standard SDS/PAGE, but sample buffer excludes 2-mercaptoethanol.

Semi-Denaturing Detergent Agarose Gel Electrophoresis (SDD-AGE)

SDD-AGE were performed as described in previously.[2,3] Briefly, 1% agarose, Tris-Acetate-EDTA (TAE), 0.1% SDS gel was cast. Cell lysates were loaded with sample buffer (0.5xTAE, 5% glycerol, 2% SDS, and 0.02% bromophenol blue) and the gel was run at 4V/cm gel length in 1xTAE with 0.1%SDS. The proteins were transferred to a PVDF membrane with TBS buffer (20mM Tris (pH 7.4) and 150mM NaCl) using capillary transfer, processed by Western blot.

Cell lysates and Immunoprecipitation

Cells were harvested, thrice washed with PBS, and pelleted by centrifugation. Cell pellets were lysed with 5 volumes lysis buffer (50mM Tris (pH 7.4), 137 mM

NaCl, mM EDTA, 1% Triton X-100, and 10% glycerol, supplemented with protease inhibitors), incubated on ice (30 minutes), centrifuged (20,000g for 12 minutes) and supernatant collected. Lysates (1mg) were incubated with 20uL anti-Flag or streptavidin agarose beads at 4°C overnight. Beads were washed 5 times with lysis buffer and and eluted with 60uL elution buffer (0.2M glycine, pH2.8) and immediately neutralized with 10% 1M Tris pH 7.4.

Cell Death Assays

(i) The CellTiter-Glo assay (Promega) was performed according to manufacturer's instruction. Luminescence was measured with a Synergy 2 machine (BioTek). (ii) For image based analysis, cells were stained with SYTOX 1uM or propidium iodide 1uM and 10ug/mL DAPI at room temperature for 10 minutes and imaged with a Cytation3 machine (BioTek). Percentage of cell death was calculated by dividing SYTOX or PI positive cells by DAPI positive cells.

Recombinant Protein Purification

Complementary DNA (cDNA) encoding full length human HSPA1A and HSPA8 were cloned into pET21b vector. Cysteine mutants were generated by site-directed mutagenesis. His-fusion proteins were purified from BL21 Escherichia coli cells with Nickel beads. Purified recombinant proteins were eluted with Buffer T/250mM imidazole and dialyzed against PBS buffer.

MLKL Polymerization

Recombinant NTD-MLKL was generated as previously described.[6] Recombinant NTD-MLKL (5nM or 200nM) was incubated with or without recombinant Hsc70 (350nM) and Hsp70 (175nM or 350nM), Hsp70 truncations or cysteine mutants (350nM) at 23°C in PBS buffer for 1 or 3 hours as indicated.

***In vitro* compound conjugation assay**

Recombinant Hsp70, Hsp70 truncations or cysteine mutants (350nM) were incubated with 0.5 µM B-NBC1 or B-NA at 4°C in PBS buffer for 16 hours.

Mass Spectrometry-Liquid Chromatography (MS-LC).

MS-LC was performed as previously described.[5] Briefly, the protein band of interest was excised, destained, and reduced followed by in-gel trypsin digestion. The peptides were extracted and analyzed by QSTAR XL mass spectrometer (AB Sciex, CA, USA).

RNA isolation, cDNA generation, and qPCR

Total RNA was isolated from NTD-DmrB cells with Direct-zol™ RNA Kits (Zymo Research). cDNA was synthesized using iScript cDNA synthesis kit (BioRad, 1708891) using 1 µg RNA. Gene expression was assessed using standard qPCR approaches with iTaq™ universal SYBR® Green supermix (172-5124). Analysis was performed on CFX Connect™ Real-Time PCR Detection System (BioRad).

The $2^{\Delta\Delta Ct}$ method was used to analyze the relative change in gene expression normalized to actin. The following primers were used for qPCR:

Hsp70-F, 5'-AGGACATCAGCCAGAACAAG-3';

Hsp70-R, 5'-CTGGTGATGGACGTGTAGAAG-3',

NTD-MLKL-F, 5'- CCCTCTGAGAAGTTAACCACAG-3';

NTD-MLKL-R, 5'- GTCCTGGCTTGCTGTTAGAA-3'.

***In vitro* metabolic stability assay**

NBC1 (2mM in DMSO) was incubated with Murine S9 (Lot KWB) fraction and Phase I (NADPH Regenerating System) cofactors for 0-240 minutes. Reactions were quenched with 1 mL (1:1) of methanol containing 0.2% formic acid and 100 ng/ml IS (IS final conc. = 50 ng/ml). Samples were vortexed for 15 seconds, incubated at RT for 10 minutes and spun for 5 minutes at 2400 rpm. Supernatant (1 mL) was then transferred to an eppendorf tube and spun in a table top, chilled centrifuge for 5 minutes at 13.2K rpm. Supernatant (800 uL) was transferred to an HPLC vial (w/out insert). Analyzed by Qtrap 4000 mass spectrometer (AB SCIEX).

Negative stain electron microscopy. Two hundred mesh carbon/formvar-coated copper grids were rendered hydrophilic by glow-discharge in air. Protein sample (5 µL) was applied to the grid and incubated for 30 s. After wicking, the samples were stained with 5 µL of 1% uranyl acetate for 1 min, wicked, and air

dried for a minimum of 15 min. Images were obtained on a FEI Tecnai G2 Spirit electron microscope.

Immunogold electron microscopy. Post-embedding immunolabeling targeted at mouse secondary antibody. Fixation in paraformaldehyde/glutaraldehye mixture followed by gentle dehydration, embedding in water miscible acrylic resin (LR Gold), and labeling of ultrathin sections. Images were obtained on a FEI Tecnai G2 Spirit electron microscope.

Statistical analysis

Statistical analyses was performed with Excel: Student's t-test was used to determine significance in cell death, $p<0.05$ will be used to determine significant differences in cell death. Data is presented as mean +/- SD.

ACKNOWLEDGEMENTS

Thank you to the Cellular and Molecular Biology training grant T32GM008203 (2014-2017) for my funding.

I would like to thank Drs. Yuyong Ma, Chengwei Zhang, and Chuo Chen for compound synthesis, the project would not have been possible without the NBC1 analogs. Thank you to Dr. Noelle Williams and Bethany Cross of the UT Southwestern Pharmacology Core for performing the *in vitro* metabolic stability assay, and the electron microscopy core, particularly Phoebe Doss, for her patient assistance with imaging.

I would also like to thank the National Institute of Biological Sciences (Beijing, China) for performing LC/MS and the NCI/DTP Open Chemical Repository for the compound libraries.

My sincerest thanks to my thesis committee, Dr. Michael Roth, Dr. Chuo Chen, and Dr. Peter Douglas, for sharing their time and expertise and offering sane guidance. Thank you also to Dr. Christopher Liu for his time on my committee and ischemia-reperfusion surgical training.

From the Wang Lab, I would like to thank Dr. Shuzhen Liu for the MLKL immunoprecipitation that identified its interaction with Hsp70 and chatting across the bench; Dr. Eduardo Reynoso for generating the recombinant NTD-MLKL protein and paving the way as the first Wang Lab student; Hong Yu for technical assistance and fashion expertise; Dr. Yougui Xiang for experimental advice and Chinese cultural information; and Sarah Hanna Addams for being a fabulous fellow-graduate student and an even better friend.

Thank you to the amazing and supportive NA8 community, especially Dr. Ebony Flowers and Dr. Berfin Azizoglu.

Most of all I would like to thank my husband, for putting up with my endless education and being wonderful.

1. Wang, Z., Jiang, H., Chen, S., Du, F. & Wang, X. The mitochondrial phosphatase PGAM5 functions at the convergence point of multiple necrotic death pathways. *Cell* **148**, 228-243 (2012).
2. Liu, S*., et al.* MLKL forms disulfide bond-dependent amyloid-like polymers to induce necroptosis. *Proc Natl Acad Sci U S A* (2017).
3. Halfmann, R. & Lindquist, S. Screening for amyloid aggregation by Semi-Denaturing Detergent-Agarose Gel Electrophoresis. *J Vis Exp* (2008).